Phoenix: Towards Designing and Developing a Human Assistant Rover

AKIB ZAMAN [1,2], **MOHAMMAD SHAHJAHAN MAJIB** [1], **SHOEB AHMED TANJIM** [1],
SHAH MD. AHASAN SIDDIQUE [3], **FARDEEN ASHRAF** [1], **SHAFAYETUL ISLAM** [1],
ABU HENA MD. MARUF MORSHED [3], **SHADMAN TAJWAR SHAHID** [3], **ISHRAQ HASAN** [1],
OLIULLAH SAMIR [3], **SAFWAN SHAFQUAT** [3], **NAIM IBNA KHADEM AL BHUYAIN** [1],
ASIF MAHMUD RAYHAN [3], **MD. MUSHFIK UL ISLAM** [3], **MD. AKHTARUZZAMAN** [1],
AND MD. MAHBUBUR RAHMAN [1], **(Member, IEEE)**
[1] Department of Computer Science and Engineering, Military Institute of Science and Technology (MIST), Dhaka 1216, Bangladesh
[2] Department of Computer Science and Engineering, United International University, Dhaka 1212, Bangladesh
[3] Department of Mechanical Engineering, Military Institute of Science and Technology (MIST), Dhaka 1216, Bangladesh

Corresponding author: Mohammad Shahjahan Majib (smajib@yahoo.com)

ABSTRACT Human-assistance rovers have a broad prospect in the field of space robotics, as a significant number of organizations and researchers have been investing in the design and development of sophisticated rovers for planetary exploration. In order to promote research and development in the design of next-generation MARS rovers, an annual University Rover Challenge (URC) is hosted by the MARS Society in the United States. In this study, we highlight the design and development process of several novel subsystems of a human-assistance planetary exploration rover and their successive integration in the prototype named PHOENIX, which is a rover that participated in the URC 2021. First, a detailed requirement elicitation has been conducted, for designing a conceptual framework for a rover capable of planetary exploration. Secondly, the design and development process has been detailed for five basic subsystems (power, communication, primary-manipulator, chassis with drive, processing) and two mission-specific subsystems (scientific exploration and autonomous navigation), as well as their successive integration into the rover. Afterwards, a detailed evaluation study has been conducted in order to validate the performance of the developed system. Terrain traversability, autonomy in navigation, and sophisticated task execution capabilities have been evaluated individually within this study. Additionally, the capability of the rover in detecting bio-signatures from soil samples using a novel Multiple Bio-molecular Rapid Life Detection (MBLDP-R) protocol has also been evaluated. The developed scientific exploration subsystem is capable of detecting the presence of life from soil samples with a 92% success rate, and from rock samples with a success rate of 93.33%.

INDEX TERMS Human assistant rover, autonomous navigation, equipment servicing, terrain traversal, planetary exploration, life detection.

I. INTRODUCTION

Space robotics is one of the pioneering sectors of robotics having a rich and successful history [1]–[3]. To date, six rovers have been sent to explore Mars, while planning is underway for a human exploration mission. A robot, capable of assisting astronauts in achieving challenging objectives in addition to gathering information regarding the environment, can be very useful. Moreover, it is difficult and risky for

The associate editor coordinating the review of this manuscript and approving it for publication was Yangmin Li [ID].

an astronaut to explore planets with a challenging terrain and hazardous atmosphere. For example, the astronaut might be unable to service equipment inside a broken on-board lander which might be prone to imminent explosion. There may also be some places, in which its impossible for an astronaut to traverse due to health hazard. A human-assistant rover with extreme terrain traversal and equipment servicing capabilities can address these limitations, thereby assisting the successfully completing the mission.

Rovers are being used today for various human assistance purposes in both domestic or industrial applications.

Nasir *et al.* [4] developed an electroencephalography (EEG) wave-controlled human assistance rover for physically impaired people. The authors collected brain data using a NeuroSky mindwave mobile 2 headset from the user and then sent the data back to the rover. Additionally, the rover contained user pulse sensing capabilities for health monitoring as well as smoke sensors for safety surveillance. On the other hand, Manikandan *et al.* [5] developed a firefighting rover that can be used on an industrial level. The authors devised a controlled dc motor nozzle configuration for a changeable flow rate of water and employed Radio Frequency (RF) and on-board camera vision to manually control the rover during fire suppression operations. On contrary, Choudhury *et al.* [6] developed an autonomous fire extinguishing rover to deal with wildfires. For the operation phase, the authors further implemented obstacle avoidance capabilities as well as a Dry Chemical Powder (DCP) cartridge fire extinguisher mechanism. Menon *et al.* [7] developed a solar-powered, autonomous monitoring rover for various agriculture-related tasks such as soil and weather parameter monitoring, fire detection, insect and pest infestation detection, etc. Banos *et al.* [8] conducted a comparative test between three robotic platforms namely wheeled, tracked, and hexapod, and found out that hexapod robotic platforms performed significantly better in terms of picking up and spreading lesser radioactive contamination during operation. Similarly, Bird *et al.* [9] developed Continuous Autonomous Radiation-Monitoring Assistance (CARMA) robot. The rover recognized and located a fixed α source embedded in the floor when the authors deployed it in a radiation active area. The findings of these studies [5], [6], [8], [9] show that human assistant rovers can be useful to replace or assist humans in risky environments. National Aeronautics and Space Administration (NASA) intends to bring Mars under human exploration mission reach within the 2030s [10]. A human assistant rover can be an excellent company with the astronaut which can assist in conducting experiments in probable hazardous extraterrestrial environments. Findings from recent studies [11]–[20] showed a trend of continuous optimization of the subsystems of human assistant rovers. Moreover, any research and development in human assistant rover for space exploration can also accelerate the development of robotics in general. As an example of this phenomenon, a well-designed robotic manipulator associated with a robot for assisting humans in space can also pave the way for developing smarter industrial robotic manipulators to drive the development of industry 4.0. A human assistant rover with the capability of traversing rough terrain can also initiate the process of developing better surveillance robot.

The University Rover Challenge (URC), organized by the Mars Society, is a premium robotics competition held yearly in the desert of southern Utah, USA, with the goal of inspiring young enthusiasts in space robotics research. URC challenges university students to design and build next-generation Mars rovers with a vision for utilizing the developed rovers to work
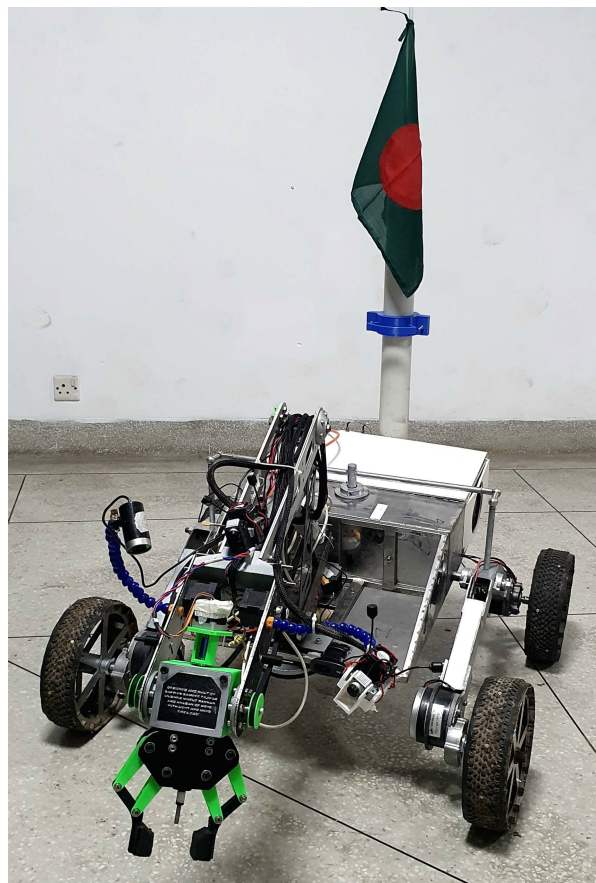

FIGURE 1. Developed Rover, PHOENIX.

alongside human explorers in the field [21]. We present the design and development of a novel human assistant rover named PHOENIX (see Figure 1) which is capable of assisting humans in planetary exploration and successfully participated in URC 2021 being evaluated in possible real life use cases.

In this study, Each aspect of design and development of the PHOENIX rover with detailed emphasis on requirement elicitation and subsystem-level conceptual framework design is explored. The requirement elicitation is conducted based on the requirements and design constraints in URC 2021. To satisfy these requirements, the overall rover system is segmented into seven subsystems. Among them, five subsystems (power, processing, primary manipulator, chassis and drive, communication) are required to avail the basic functionality of the rover. The other two subsystems (scientific exploration and autonomous navigation) are mission-specific and modular in nature, as they can be attached and swapped with each other, depending on mission requirements. The successive integration of these subsystems into the rover, as well as their performance analysis are also highlighted in this study.

In this study, A comprehensive requirement elicitation is conducted to design a subsystem level conceptual framework of a human assistant rover to demonstrate planetary exploration capability in URC 2021. The requirement elicitation is based on URC 2021's requirements and design restrictions

and the whole rover system is divided into seven subsystems to meet these objectives. Five subsystems are required to provide the rover's fundamental operation (power, processing, primary manipulator, chassis and drive, and communication). The other two subsystems (scientific exploration and autonomous navigation) are mission-specific and modular, meaning they may be joined to and changed out depending on mission needs. This research focuses on the gradual integration of these subsystems into the rover, as well as their performance assessments. A thorough evaluation is conducted on the rover, in scenario-based tests, with sophisticated tasks such as "tightening screws", "typing on a keyboard", etc. which require fine-grained control of the end-effector. Moreover, tests regarding the robustness, navigability, traversability, and other mechanical capabilities of the rover are also conducted in the evaluation phase. The rover also successfully traverses autonomously to a target location by localizing itself and planning a route towards the goal using the developed autonomous navigation system. Additionally, in the science subsystem a novel Multiple Bio-molecules Based Rapid Life Detection (MBLDP-R) protocol is developed to detect bio-signatures on-board from soil samples, as well as a deep learning and sensor infusion based life-detection protocol from rock samples. In summary, the work contains the following contributions:

- We conduct a multi-disciplinary research that bridges between robotics and detection of life in space.
- We develop a subsystem level conceptual framework of a human assistant rover capable of conducting planetary exploration.
- We develop a novel five Degree Of Freedom (DOF) primary manipulator with the inclusion of semi-differential wrist mechanism, which is capable of lifting payload up to 7 kg and perform various sophisticated equipment servicing tasks.
- We develop an intelligent path planning strategy with the integration of GPS data into Simultaneous Localization And Mapping (SLAM) algorithm to navigate the rover autonomously.
- We develop a novel scientific exploration subsystem which is capable of soil sample collection and on-board analysis.
- We develop a novel multiple Bio-molecules Based Rapid Life Detection Protocol (MBLDP-R) to detect presence of life from a soil sample and a novel protocol using deep learning and sensor data infusion to detect presence of life from a rock sample.
- We successfully integrate the developed subsystems and constructed a human assistant rover for planetary exploration.
- We present experimental result to show the performance of the developed system by conducting a detailed evaluation study.

The remainder of the paper is structured as follows: section II describes the development of the subsystem level conceptual framework of the system using the findings of prior works and requirement elicitation. The design and development of various subsystems of the rover is described in section III to VII. Evaluation of the developed features and capabilities of the rover in a controlled environment is highlighted in Section VIII. Finally, section IX summarizes the work along with its limitations and future scope.

II. DEVELOPMENT OF CONCEPTUAL FRAMEWORK
A. URC 2021 REQUIREMENT ANALYSIS
1) GENERAL SYSTEM REQUIREMENTS
The system requirements are set as per the guidelines and constraints of URC 2021. According to the guidelines, rovers are not expected to travel more than 1 km from the command station and should be functional at moderate day temperature (100°F). For weighing, the rover must fit completely within a 1.2 m x 1.2 m box. The maximum allowable mass of the rover when deployed for any competition mission is 50 kg. (The combined mass of the rover with the attached primary manipulator, or with scientific exploration subsystem must be under 50 kg, but the total of all the subsystems must be less than 70 kg). Moreover, modularity is encouraged in the case of building the overall system as the configuration of the rover can be different in missions.

2) COMMUNICATION SUBSYSTEM
The primary requirement of the communication subsystem is a minimum effective range of 1 kilometer, with a maximum base antenna height of 3 meters. 900 MHz, 2.4 GHz and 5 GHz bandwidth are allowed with exceptions such as a) Teams would not use frequency bandwidths greater than 8 MHz and must operate exclusively within each of the following three sub-bands: "900-Low" (902-910 MHz), "900-Mid" (911-919 MHz), and "900-High" (920-928 MHz); b) Teams would not use frequency bandwidths greater than 22 MHz in case of 2.4 GHz frequency band and were allowed to use spread spectrum or narrow band (fixed channel allocation) within the sub-band limits as they fit.

3) POWER MODULE
Rovers can utilize power and propulsion systems that are applicable to operate on Mars. Air-breathing systems are not permitted. A "kill switch" is compulsory to be readily visible and accessible on the exterior of the rover as a safety protocol and should be capable of immediately ceasing all power draw from batteries in the event of an emergency (e.g. battery fire). Battery back-up is expected for a minimum period of 30 minutes to a maximum period of 60 minutes.

4) SCIENTIFIC EXPLORATION SUBSYSTEM
The rover is expected to determine the absence or presence of life (either extinct or extant) for designated samples on-site, using only the on-board science exploration subsystem. The rover is allowed to collect soil samples for on-board analysis but no rock samples are allowed to be removed or altered.

On-board chemicals are expected to follow a no-spill policy that keeps them contained on the rover. Each team is assigned a 30-45 minute time limit to complete the data collection needed in this mission.

5) PRIMARY MANIPULATOR SUBSYSTEM

The primary manipulator is not being restricted by any measurements; rather, the given missions are the main factors to consider when designing it. Objects to be retrieved in the field consisted of small lightweight hand tools (e.g. screwdriver, hammer, wrench), supply containers (e.g. toolbox, gasoline can), or rocks up to 5 kg in mass. All items except the rocks had graspable features (such as a handle) no greater than 5 cm in diameter, while the maximum dimensions are no larger than 40 cm x 40 cm x 40 cm. The rover is required to pull one object, weighing less than 5kg, by a rope over the relatively flat ground towards itself and then pick it up. The rope's dimensions are 15mm in diameter and 3 meters in length. A panel of an imitation lander rocket is provided for the equipment servicing mission. The lander had drawers and equipment panels fitted onto it. The rover is required to pick up a cache weighing less than 3 kg, open the drawer on the lander and put the cache in it. The rover must be capable of tightening a 5/16'' Allen (hex) head screw. Additionally inserting a USB memory stick into a USB (type A) slot, writing a specific word using a mechanical keyboard, operating flip switches and operating a joystick to direct an antenna should be handled by the primary manipulator of the rover to demonstrate equipment servicing capability.

6) AUTONOMOUS NAVIGATION SUBSYSTEM

In this staged mission across easy to moderately difficult terrain, the rover is expected to autonomously traverse to posts or between gates based on specified GPS coordinates. Each post would have a large (20cm × 20cm) marker 30–100 cm off the ground. Each gate would consist of a pair of posts 2-3 m apart. Each marker would display a black and white AR tag, which is needed to be identified by the rover upon arrival near the posts. Obstacles in the route would be sparsely distributed in phase 2 of the two-phased expedition. The rover is needed to identify the obstacles and traverse around them to reach the posts autonomously. There must be an LED indicator on the back of the rover, visible in bright daylight that would signal three different colours a) Red (Autonomous); b) Blue (Manually driving); c) Flashing Green (Successful completion of the manoeuvre). The rover's processing unit is required to decide when it had reached a post or passed through a gate. The rover must then stop and signal the completion of a leg using the LED indicator (flashing Green light). It must also display a message or signal on the operator's display for the control station to be observed by the judges.

B. PRIOR WORKS

Since the start of 2006, URC featured a good number of well-constructed rovers in each year and several works were documented as a research publication. J. Rozsa *et al.* developed a six-wheel BYU Mars Rover [22]. The rover used a directional antenna housed on a custom rotating antenna mount which enabled it to handle line-of-sight communications. Additionally, theora compression and resolution limiting was used for managing video latency. Though the rover was effective in radio-telemetry operations, no specific subsystem related to autonomous navigation, primary manipulator operation and science mission operations were mentioned in the research. Similarly, T. Bernard *et al.* [23] developed a six-wheel rover consisting of three main subsystems: the rocker-bogie suspension, the counter-rotating differential and a base plate that houses both the electronic equipment and the custom-designed robotic arm of the rover. Bearing a truss structure, the robotic arm had three linkages: a shoulder, an elbow and a wrist link with a custom-built end-effector at the extremity of the wrist link with six operational degrees of freedom (DOF). For the autonomous traversing, the rover used an auxiliary UAV (Unmanned Aerial Vehicle) attached to the body, which provided regional information of the surrounding terrain of the rover during traversal. Moreover, the UAV was designed primarily to work alongside the rover in the astronaut assistance and delivery mission. During the mission, the rover would pick up a tool and the UAV would then deliver that tool to the designated delivery point. This mixed usage of UAV and rover greatly increased the teams' mission time efficiency. The UAV would also be used for surveillance to locate objects or soil samples for the science mission and identify optimal travel paths. However, no specific subsystems for autonomous navigation and scientific sample or habitability analysis were developed. Uday et. al developed UIU Mars Rover [24], a six-wheel, modified rocker-bogie, autonomous robotic system. Criss-cross bars were used on the rover chassis for absorbing unbalanced pressure and differential drives system for both reducing the turning radius and increasing the speed of the rover. The rover arm consisted of two links, three joints and one actuator stroke of 100 mm with five operational degrees of freedom and two end-effectors. The rovers' network stack design provided reliable speed and bandwidth using an 8 dBi antenna on the rover and a 24 dB grid parabolic antenna at the ground station. Though the rover was capable of in-situ soil habitability analysis by analyzing on-board sensor data such as soil moisture, UV exposure, ambient temperature, humidity and presence of toxic gases, in-situ life detection from soil or rock analysis was not developed. M. Gajewski et. al. [25] developed Sirius, a four-wheeled autonomous rover. The rovers' manipulator consists of a rotating base, 3 staged arms and an end effector. The rotation and movement of the manipulator were done using two motors with gearing and two linear actuators. Two different end effectors were designed, one with parallel moving fingers and one with fingers closing on an arch path. For the autonomous traversal, on board ultrasonic sensors, IMU sensors, and RGB cameras were used.
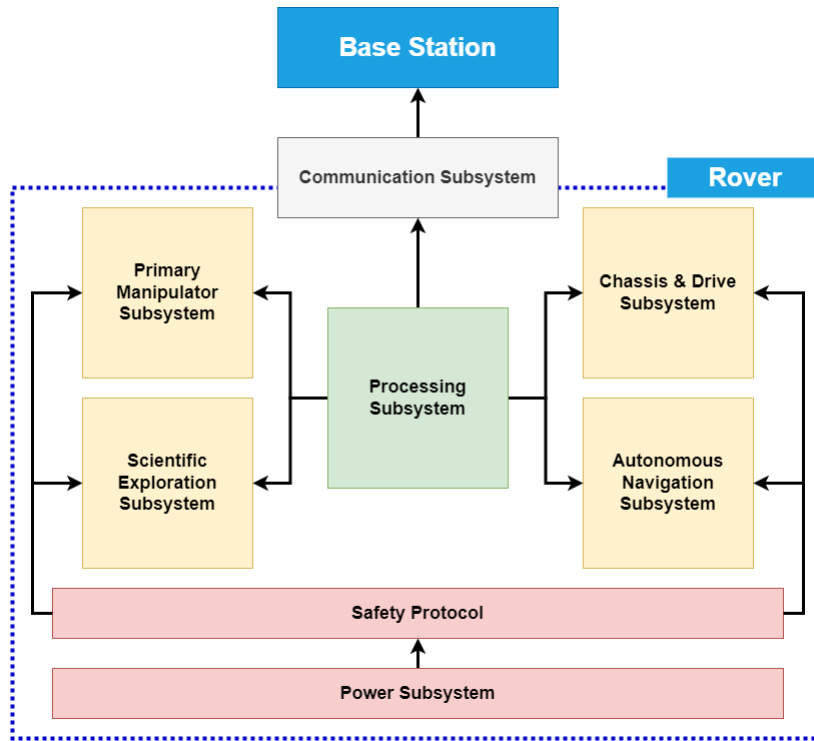
FIGURE 2. Conceptual Framework (Subsystem-level) of the System.

C. EXTRACTION OF BROAD LEVEL DESIGN OF THE SUBSYSTEMS

From the extracted requirements and findings of prior works, a subsystem-level conceptual framework of the rover (see Figure 2) is developed. The framework consists of five basic subsystems (power, processing, primary manipulator, chassis and drive, communication) and two mission-specific subsystems (scientific exploration and autonomous navigation).

The communication subsystem establishes a stable connection between the base station and the rover. We worked on the assumption that a long range communication module based on a lower frequency would be a decent solution. For inter subsystem communication inside the rover, a packet switching device was assumed to be a viable approach. Additionally, it would be necessary to formulate an algorithm (see Algorithm 1) for communication among the subsystems within the rover, as well as the transmission of data from the rover to the base station and vice versa.

The processing subsystem would be regarded as the central core of the rover, since the information from all the subsystems are processed here for general rover operations, mission-specific operations and primary manipulator operations. The processing subsystem is directly connected with four subsystems: primary manipulator, chassis & drive, autonomous navigation, and scientific exploration subsystems. This subsystem is required to be capable of handling and assessing a sufficient amount of outgoing & incoming data to provide different computational decisions. Thus, the NVIDIA Jetson platform was chosen as a viable candidate for the processing

needs due to it's decent computational capabilities and minimal form factor.

On the other hand, the chassis and drive subsystem is designed with the objective of enabling the rover to operate on rough terrain and carrying other subsystems with it while doing so. The system is necessary to be modular so that mission-specific subsystems can be quickly attached or detached to the chassis and drive subsystem of the rover. Initially, we assumed that a six-wheel rocker-bogie suspension mechanism with differential bar would satisfy the requirement of traversing a challenging terrain. To conform with this assumption, we decided to develop a five DOF primary manipulator system to perform pick-and-place operations in equipment servicing and extreme retrieval-delivery missions. Alongside pick-and-place operations, several sophisticated features like tightening a screw, inserting a USB drive in the slot, etc. were kept into consideration while designing the manipulator. Keeping these requirements in consideration, a three bevel gear-meshed semi differential wrist mechanism, as well as a parallax gripper was designed, in order to ensure the required flexibility and precision while performing the mentioned sophisticated tasks.

The autonomous navigation subsystem enables the rover to traverse the terrain without any radio-telemetry commands given from the base station. The subsystem also needs to detect obstructions in the field and change its course of navigation in accordance. For strategic path planning and obstacle detection, we decided to use a depth-sensing camera, along with a 2D laser scanner. Incorporating GPS data with

---

Algorithm 1 Algorithm of Rover Control System of PHOENIX

---

1 Start the Rover;
2 Connect with the Base Station;
3 **while** *Receives the signal from Base Station* **do**
4   **if** *Rover movement command* **then**
5   Drive the Rover ;   `/* Drive Subsystem */`
6   **else if** *Manipulator movement command* **then**
7   Move the manipulator ;   `/* Primary Manipulator Subsystem */`
8   **else if** *Autonomous command* **then**
9   Waits for the goal information ;   `/* Autonomous Subsystem */`
10   Drive to the goal autonomously and send back telemetry data ;
11   **if** *Reach to the goal successfully* **then**
12   Send a success status back to the base station;
13   **else if** *Error occurred* **then**
14   Send the error info back to the base station;
15   **else if** *Science command* **then**
16   Waits for receiving the task sequence ;   `/* Science Subsystem */`
17   Execute the task ;
18   Sends rover sensor data back to the base station;

---

the data obtained from these sensors, allowed us to design the autonomous navigation framework. To filter and process the data, we customized various existing packages of Robotic Operating System (ROS). NVIDIA Jetson platform provided a decent platform for running ROS and conducting the necessary resource-heavy computations.

The power subsystem provides the necessary power to all the other subsystems. The input of the power subsystem is required to be passed through a safety protocol providing a layer of security from voltage surges, short circuits, etc. A Commercial Off-The-Shelf (COTS) industrial-grade switch was selected as the emergency stop button to provide safety from accidental uncontrolled movement.

Finally, the scientific exploration subsystem is a mission-specific modular subsystem with the primary goal of determining traces of biological life signatures from soil and rock samples. While adhering to a no-spill policy, the subsystem should be capable of carrying different biochemical reagents on-demand, as well as conducting the biochemical soil tests on board. We considered a secondary manipulator with a drill bit like an end effector to be integrated with this subsystem to collect soil samples. For the rock samples, as the rover is prohibited from altering the rock specimens, the subsystem should have sufficient onboard microscopic examination and computer vision capabilities for analyzing outer rock surfaces. Furthermore, the rover should be able to detect various algae, bacterial, and fungal specimens that may be present on rock surfaces using various micro-Volatile Organic Compound (mVOC) detecting sensors. The capabilities indicated above for the scientific exploration subsystem are expected to be sufficient for detecting extinct, extant, and NPL from soil and rock samples.

III. ROVER MECHANICS

PHOENIX is constructed in two different configurations: a) Chassis with primary manipulator subsystem and b) Chassis with scientific exploration subsystem.

A. CHASSIS AND DRIVE SUBSYSTEM

At first, a six-wheel locomotion system (see Figure 3(a)) was designed to utilize the rocker-bogie suspension mechanism of the rover to its full extent. The rocker-bogie mechanism allows all the wheels to contact the ground during movement over any rough terrains. This enables the total body weight to be distributed across all wheels, ensuring stability and improving the overall performance of the system. The six-wheel design featured a U-shaped joint that attached the motor to the rocker-bogie mechanism. The objective was to mount the motors inside the wheel frame to distribute the reaction force to a suitable position. However, it was observed from the static structural analysis (see Figure 4) that, the U-shaped joint absorbs a large portion of the turning torque by deforming and hindering the turning motion. Also, excess traction was required to rotate a six-wheel rover which requires high torque and thereby consumes a higher amount of power. Moreover, the rotation was jerky and uncontrolled.

To address these limitations, a new design with four wheel architecture is proposed. We conduct a deformation and strain analysis on the bogie of the first version and on the wheel frame of the second version of the rover keeping the pivot bar as a fixed support. The simulation was done based on the equation 1 where E denotes elasticity, σ denotes stress and ϵ denotes strain.

$$E = \frac{\sigma}{\epsilon} \qquad (1)$$
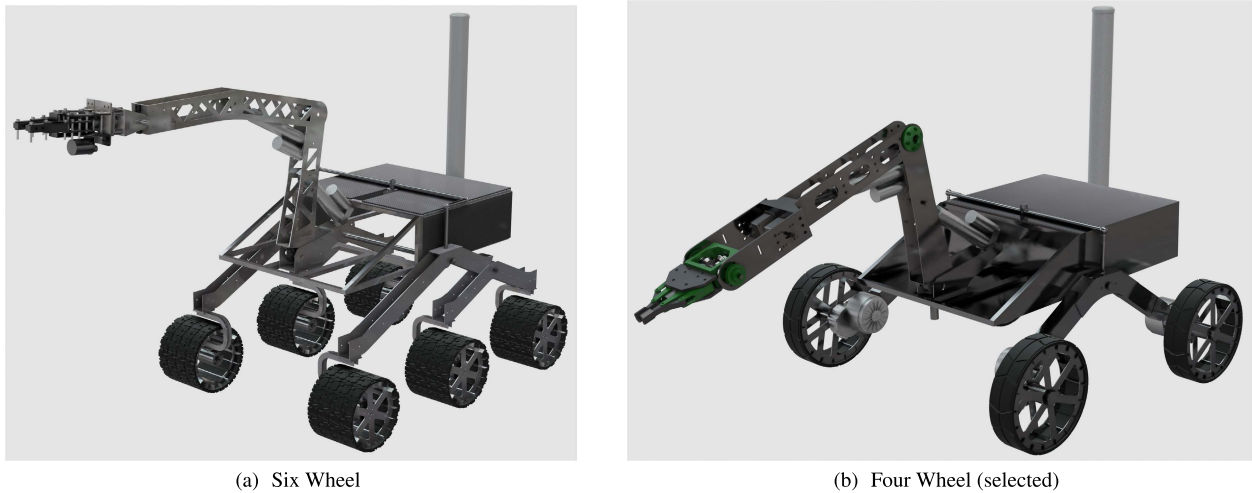
(a) Six Wheel   (b) Four Wheel (selected)

FIGURE 3. CAD of Chassis and Drive Subsystem with Primary Manipulator.
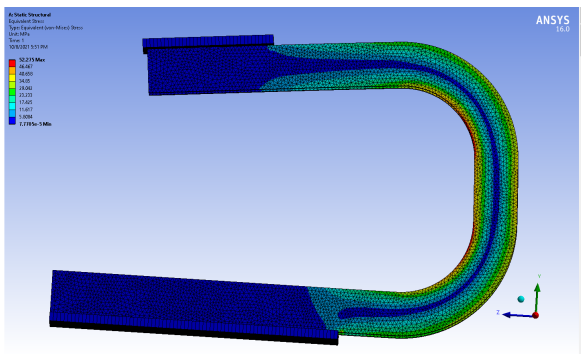
FIGURE 4. Equivalent stress analysis of U-shaped joint of the six-wheel design.

It is observed from the deformation analysis (see Figure 5) that the maximum deformation under the critical load with a safety factor of 4 is 0.17 mm and 0.16 mm respectively. But significant change is found in strain analysis (see Figure 6) that maximum strain in the first version is found in the bent portion of the bogie, which leads to buckling. In the second version however, the maximum strain is observed at the bottom of the wheel frame, which is certainly not a critical position. This frame can tolerate the reaction force without developing any buckling and the rover can withstand impact using a four-wheel mechanism. Thus, a four-wheel chassis and drive subsystem was designed (see Figure 3(b)) with a semi-differential mechanism on the body which ensures maximum ground contact, preventing the rover from tipping at the pivot during extreme traversal.

The differential bar is mounted on the chassis using a roller bearing, allowing itself to rotate along the vertical axis. The bar is connected to each wheel frame via two ball joints. To ensure strength and stiffness, the wheel frame is straddle mounted on the hardpoints of the chassis, which would be critically evaluated using structural analysis. Removing the U-shaped joints resulted in the reduction of the overall weight of the rover. Additionally, a simple plate bolted to the wheel frame is used on which the motor is mounted. For the rover to endure the bending motion, the central bearings are straddle-mounted and braced.

The dimension of the chassis and drive subsystem is 1050mm (length)×1050mm(width)×750mm (height). The chassis is built using the combination of AISI 304 Stainless Steel (SS) and Aluminum by considering the lightweight and rigidity of the materials. Custom 3D printed antenna mount, circuit box and casing are modelled using Polylactic Acid (PLA). The weight of the entire body is distributed to four supports and static structural analysis is conducted to determine proper weight distribution. Wheels (see Figure 7) are attached to the other end of each mobility support to ensure robust mobility. Four custom-built SS rims with styrene-butadiene polymer tires are developed to design the wheels. The diameter of each wheel is 260mm. SS rims are capable of carrying heavy loads and asymmetric tires with a combination of different tread patterns helped in better traction control and stability while moving on uneven surfaces. Part of the chassis was designed so that modular attachments, such as primary manipulator or scientific exploration subsystems could be easily integrated with the chassis according to mission specified requirements.

B. PRIMARY MANIPULATOR SUBSYSTEM
We have developed two different versions (see Figure 8) of the primary manipulator with five Degrees Of Freedom (DOF). Afterwards, we analyzed the performance and stability of each manipulator in scenario-based tasks involving fine-tuned control and retrieval, before selecting the optimal option. As these variants were implemented in sequence, the versions have been marked as version 1.0 (see Figure 8(a)) and version 2.0 (see Figure 8(b)) (The subsystem consisted of five major modules: a) Shoulder, b) Biceps, c) Forearms, d) Wrist and e) End-effector. The shoulder, biceps and
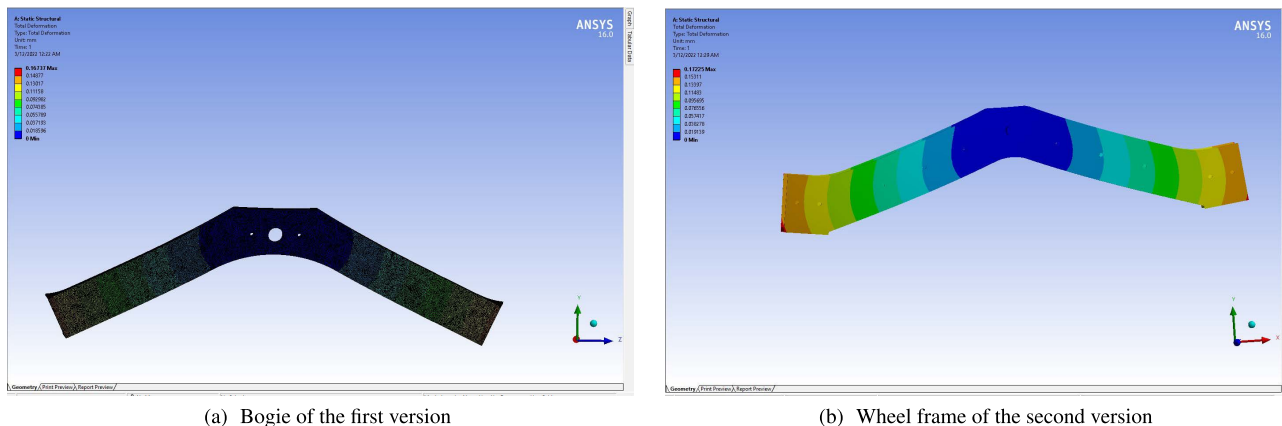
(a) Bogie of the first version

(b) Wheel frame of the second version

FIGURE 5. Deformation Analysis.

(a) Bogie of the first version

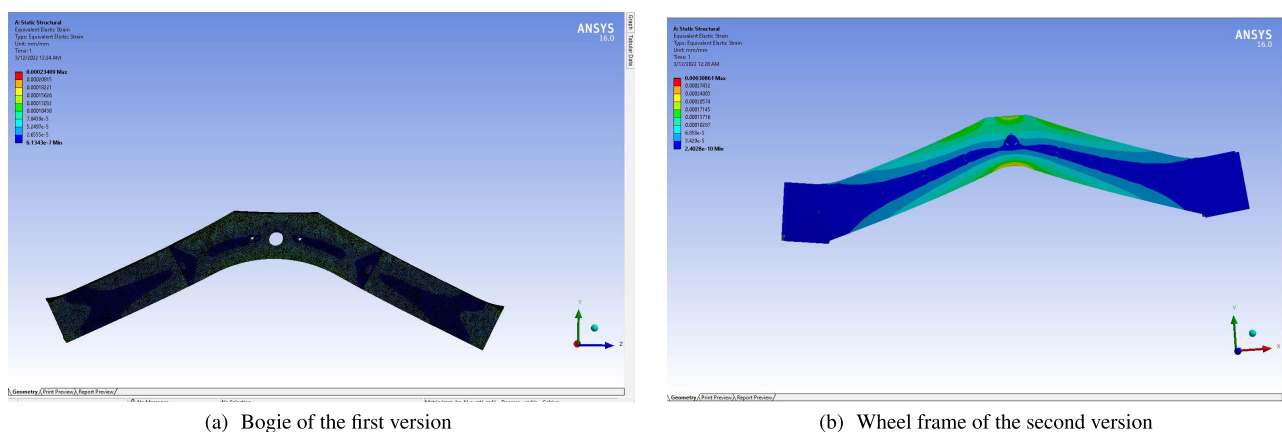
(b) Wheel frame of the second version

FIGURE 6. Strain Analysis.

forearm are similarly structured in both versions. The limitations in the wrist and end-effector modules of version 1.0 is addressed in version 2.0 and finally version 2.0 is manufactured for the rover.

1) SHOULDER

The shoulder, being the first major piece of the manipulator, anchors the entire arm to a robust foundation below it. The structural bracket consists of four CNC cut Stainless Steel (SS) metal plates welded together. The bracket, consisting of two revolute joints, is attached with a bicep and a bicep actuator. A shaft is welded with the bottom plate of the bracket, which is driven by a stepper motor. A 1:9 pulley system was also installed in order to reduce the speed and increase the torque. As the shoulder experiences some of the largest forces and moments, 3 mm SS was used, as it ensures that the shoulder would be robust and capable of handling these forces. The red-highlighted part of Figure 8(b) exhibits the shoulder.

2) BICEP

The lower region of the bicep is latched with the shoulder by a pillow block bearing of 10 mm bore diameter. The housing
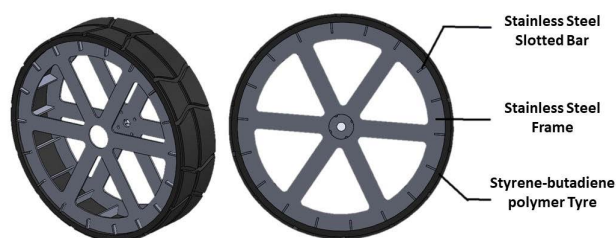

FIGURE 7. Wheel.

is 3D printed to fit the SS built CNC-cut plates of 2 mm thickness. The housing is fastened into the shoulder with six Allen head screws of 5 mm diameter. The bicep plates are attached to the shafts which fitted into the bearing bore. A 3 piece welded joint of stainless steel is also fastened by two nuts over the bicep to hold the shaft upon which the forearm revolves. The yellow-highlighted part of Figure 8(b) showcases the bicep.

3) FOREARM

The forearm is allowed to maintain a revolute joint with the bicep. CNC cut Aluminium sheet of 4 mm thickness
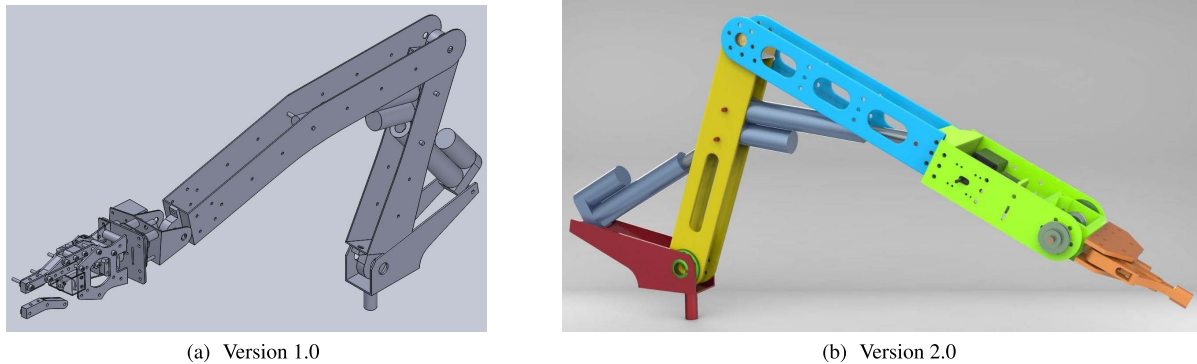
(a) Version 1.0

(b) Version 2.0

FIGURE 8. CAD of 5-DOF primary manipulator.

is used here. Its straddle is mounted via two bearings of 10 mm bore diameter. The bearing housings are 3D printed and mounted on the plate with 6 Allen head screws of 5 mm. The blue-highlighted part of Figure 8(b) exhibits the forearm. After Finite Element Analysis (FEA), von Mises Stress on forearm is located. From this simulation, the effect of various cutout patterns on the structural elements are ascertained and the most optimum pattern was chosen. This pattern is capable of overcoming loads greater than what the design requires.
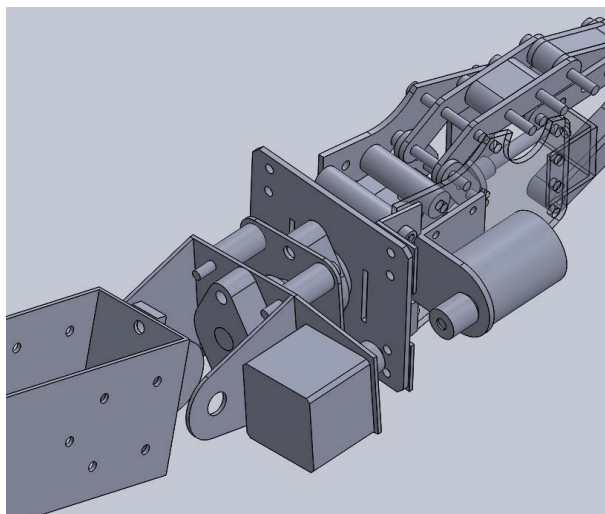
4) WRIST

The wrist is the most vital piece of the manipulator, as it possesses two major DOF (pitch and yaw). The main purpose of the wrist, in our task, is to move an object to a specified orientation. Our rover was required to do some servicing tasks like tightening screws, driving a joystick, typing on a keyboard, etc. The wrist is essential for the fine-tuned control required for these tasks. The structural bracket of the wrist consists of three CNC cut metal plates welded together. The actuation system of the wrist was initially different. In the initial actuation system, a stepper motor was mounted at the outer portion of the bracket, which would drive the pulley at the center of the bracket. That, in turn, provided the 360° yaw movement to the end effector. Additionally, a high torque DC motor was mounted at the upper portion of the forearm, which provided the pitching movement. A 1:4 chain system was also installed, in order to reduce the speed and increase the torque. Figure 9(a) exhibits the first version of the wrist.

The first version of the wrist had several limitations. The movement of the revolute joint before the wrist was provided using a DC motor. This motor weighed around 330 grams and was mounted to one side of the forearm via a chain-sprocket mechanism (speed was also needed to be reduced). As there was no scope for attaching a tensioner, the chain was required to be kept on high tension within the sprockets. This tension caused an overall buckling on the forearm as well as the bicep. The bearing in between faced considerable shear and had misalignment possibilities with this one-sided actuation. The frame of the wrist was manufactured with mild steel for the ease of welding. Mild steel was too heavy for this part of the arm and it generated buckling, as usual.

To address the limitations of the first version, a second version of the wrist (see Figure 9(b)) was developed. Initially, individual stepper motors were used for dedicated control each motion of the arm mechanism. However, incorporating stepper motors introduced excess weight and complexity to the system. A semi-differential mechanism was later introduced, using bevel-gears at the tip. This was done to make the system more compact. The translation and rotational motion of the arm is achieved by only rotating the bevel-gear using a single motor. Aluminum plates were used to reduce the weight of the wrist. A semi-differential mechanism with three bevel-gears meshed with each other was installed for providing changes to the pitch and yaw (see Figure 9(b)). A 3D-printed gearbox was used to house the gears. Two sister gears of this gear-set are connected with pulleys via shafts of non-uniform diameter. The shafts are straddle-mounted by roller bearings attached with gearbox and a 3D printed housing which resolved the problems that stem from shear stress and misalignment roller bearing in the previous version. Two stepper motors were installed in a suitable position to drive the pulleys attached with the sister gears. Here, rotating the sister gears in a similar direction provides us with the pitch movement, and rotating the gears in the opposite direction provided the yaw movement. This yaw movement turns the end effector by 360°. The middle bevel gear of the gearbox is connected with the end effector by a hollow shaft, which is kept hollow to make a path for another shaft. The latter shaft actuates the grasping mechanism of the end effector. Figure 9 exhibits the whole wrist and the green-highlighted portion of Figure 8(b) shows its position.

5) END EFFECTOR

The end-effector is a parallax gripper with tips specifically optimized for the tasks required. All of the links are 3D printed with PLA material enclosed by CNC-cut aluminium plates and the links are kinematic bounded so that the flat surface of the two tips always remain parallel to each other. In order to meet the requirement of high torque at the tip, a worm gear mechanism was installed. A stepper motor is mounted at one side of the end-effector to drive the pulley which is connected with the worm gear. A 3D printed block

(a) Version 1.0

(b) Version 2.0

FIGURE 9. **Wrist of the Primary Manipulator.**

meshed with the worm gear is actuating the links by moving itself linearly up or downwards. Figure 10(a) illustrates the first version of the end-effector.

The first version of the end-effector showed several limitations. The gripping motion of the end effector was provided with a stepper motor positioned at one side. The addition of this stepper motor shifted the mass-centre. Moreover, the rotational speed provided by the motor was not uniform as no counter-weight at the opposite side was added to balance the motion. Additionally, the wire of the stepper motor at the end effector got tangled after only 4 to 5 rotations. Again, a longer wire could not be deployed as it would have lessen the range of motion by getting into the traversing region of the arm. Additionally, 3D printed spacers enclosed in between aluminum plates were bolted in place, which increased the weight of the end-effector. Again, due to the use of different types of materials, there was no alternative way to settle the gap except bolting it down.

To address the limitations of the first version, a second version of the end effector is developed. The majority portion of the gripper is 3D printed to allow for a more simple build consisting of only ten major parts. Bearings are used at the bottom parallel links with 5mm screws used as shafts as well as structural elements simultaneously. The gripper is designed to lift a 5 kg load against gravity and as such needs to produce large torque at the gripper tips. Hence, a worm gear-wheel mechanism is employed to acquire high torque (see Figure 10(b)). The worm gear is made of SS since 3D printed worm gears show wear after a few cycles. The worm wheel is incorporated in the upper parallel link itself and can be 3d printed as they are less prone to wear. The mechanism is actuated by a stepper motor placed below the differential housing of the wrist. This helped to overcome the above stated problems of first version, creating better wire management and proper weight distribution of the end

effector. Finally, the tip is fitted with a compliant material to prevent damaging the object when held. Figure 10 exhibits the whole end-effector of both the versions and the orange-highlighted portion of Figure 8(b) shows its location.

C. SCIENTIFIC SUBSYSTEM
Scientific Subsystem is developed with a 4-DOF mechanism. The subsystem is divided into two primary modules: a) Secondary Manipulator, b) On-board Soil Sample Analysis Mechanism. The subsystem is designed (see Figure 11(a)) with the consideration of the requirements of the science mission and flexible integration with the chassis subsystem. The subsystem is capable of collecting 4 soil samples at a time, conducting on-board tests for the detection of multiple biomolecules (protein, carbohydrate and ammonium ion) from soil samples, capturing high-quality images of rock samples to classify them and analyse the habitability of a sample area.

1) SECONDARY MANIPULATOR
Secondary manipulator has three DOF (see Figure 11(a)) with a multi-functional end effector. The drill bit at the end effector is made of mild steel with approximately 100 mm in length and the outer diameter is 35 mm. Linear bearings with 3D printed housing are used to ensure smooth motion and linear rods of 8 mm diameter are used to support the stainless-steel plates. To drive the manipulator, two square threaded lead screws of 8 mm diameter are used to collect soil samples from the ground and to place it in the beaker for further operation. Two separate stepper motors (NEMA 17) drive the lead screws. A 5 × 8 coupler connects lead screws and the stepper motors. Using a lead screw mechanism, the manipulator can move along the X and Z-axes and the end effector rotates along the Z-axis to collect the soil samples. For preventing cross-contamination, a liquid sanitization mechanism is added with the end effector releasing a flow of
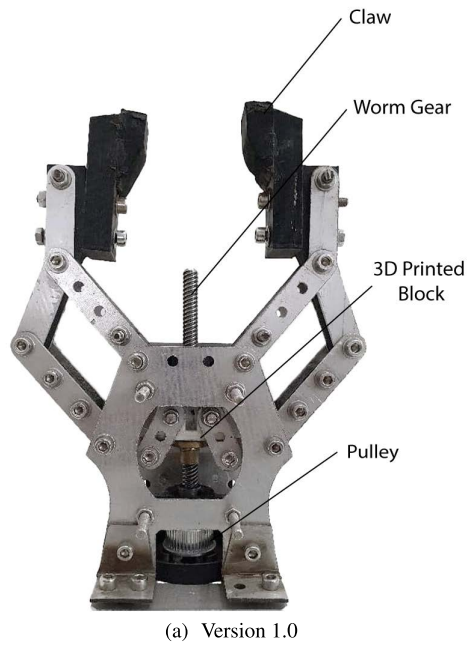
(a) Version 1.0
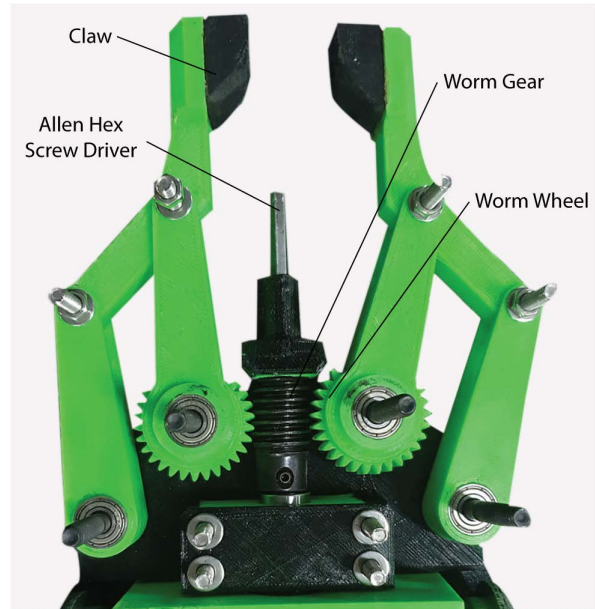
(b) Version 2.0

FIGURE 10. End Effector of the Primary Manipulator.

hydrogen peroxide after each sample collection. On top of the end effector, a 3D printed panel is constructed for holding the main camera, the USB microscope and multiple sensors (TCS3200 RGB Color sensor, MQ137 Ammonia Detection Sensor, MQ135 Air Quality Sensor Module for CO_2 detection, MQ3 alcohol sensor and MQ138 Formaldehyde Detection Sensor) as shown in Figure 11(d). The mentioned sensors are installed for the detection of life in the rock samples and analysing the habitability of a sample area.

2) ON-BOARD SOIL SAMPLE ANALYSIS

The on-board soil sample analysis module is capable of storing the soil sample and conducting chemical tests to detect the presence of life from the soil samples. The sample collection chamber consists of 12 (borosilicate glass) beakers, a 2.5 mm thick aluminium-holding frame, and a heat source. The frame alongside the beakers can move back and forth along the Y-axis to collect samples. Samples are arranged along the Y-axis and the concurrent biomolecules tests are planned along the X-axis as shown in Figure 11(b). A customized heat-pad is used as a heat source capable of generating 3600 Watt/hr energy for providing necessary heat for the tests. The reagent flow mechanism consists of three containers containing the reagents of the selected tests, a litmus mechanism for ammonium test, and 1 DOF tube framework. As per the selected tests, the containers are filled with Benedict's reagent (carbohydrate test), Ninhydrin reagent (protein test), Sodium Hydroxide solution (ammonium ion test), and strips of litmus paper (ammonium ion test). Three-12V DC Diaphragm Metering Miniature Short Motor Water Pumps deliver the reagents. The implemented subsystem attached with the chassis is shown in the Figure 11(c).

IV. ROVER ELECTRONICS

The system architecture of the robot is illustrated in Figure 12. Enhanced modularity in the processing subsystem is one of the advantages of the developed rover. The processing subsystem can be broadly divided into four modules; a) Drive, b) Primary Manipulator, c) Autonomous Navigation and d) Scientific Exploration. These modules maintain internal communication with each other through a 8-port switch or with the base station via the communication subsystem elaborated in the later section.

An Arduino Uno is used as the main processing unit in the drive module. Three Sabertooth motor drivers (Sabertooth dual 32A motor driver) are used to drive the four DC Geared motors (250 Watt My1016Z2) attached with the wheels. Additionally, for controlling the movement of the rover, Blacksheep Rx is integrated with the processing unit. A First Person View (FPV) body camera functions as the main vision of the rover, and an IP camera is set up for monitoring the wheels that are independently powered (12V) by the developed power module. The temperature, current and voltage sensors are integrated for collecting the internal status of the rover.

In the case of the primary manipulator, an Arduino Mega is used as the processing unit. 2 Motor drivers (BTS7960) are used to control the movement of actuators. A NEMA 34 stepper motor driver is used to control the base of the manipulator and two NEMA 17 motors to control the movement of the wrist and end effector, using the bevel gear mechanism. Additionally, two FPV cameras are used as the wrist and end-effector cameras to capture the side view and top view of an element respectively.

An NVIDIA Jetson Xavier NX is used as the master processing unit of the autonomous navigation subsystem.
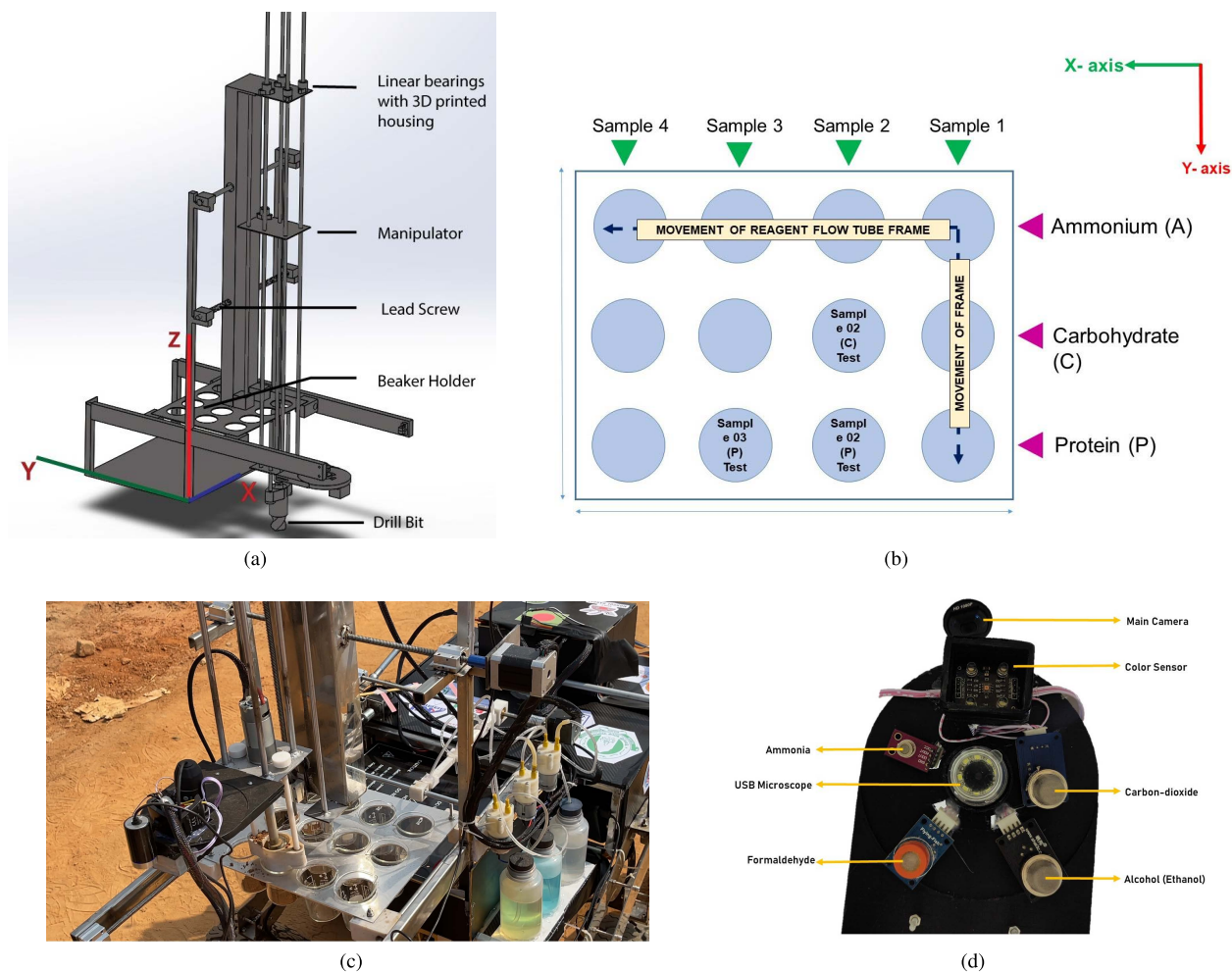
(a)

(b)

(c)

(d)

FIGURE 11. Scientific Exploration Subsystem (a) CAD Design (b) Mechanism of the on-board analysis (c) Implemented subsystem attached with the chassis (d) sensor setup in the end-effector of secondary manipulator to analyse rock sample.

A depth-sensing camera (ZED-2) and a LIDAR sensor (RPLidar A2) are integrated with the master processing unit. An Arduino Nano is used as a relay between the Jetson and the GPS modules which acts as a buffer for the GPS data.

The scientific Exploration module consists of three processing units. An Arduino Mega is used as the processing unit for the maneuvering the secondary manipulator, as well as move the soil collection chamber. Multi-functional motor drivers are integrated with the processing unit for executing various tasks such as movement of the reactant-flow mechanism (one stepper motor driver), movement of the secondary manipulator (two stepper motor drivers), movement of the soil collection chamber (one stepper motor driver), movement of the end effector to collect soil sample (one BTS motor driver) and movement of litmus strip test bar (one servo motor driver). For the rock sample test, 4 mVOC sensors (MQ137 Ammonia detection sensor, MQ135 air quality sensor module for CO2 detection, MQ3 alcohol sensor, MQ138 formaldehyde detection sensor) and a RGB colour sensor (TCS3200) are integrated with another Arduino Uno. This processing unit is directly connected with the switch for

sending the sensor data to the base station via the communication subsystem. Similar to the Arduino-Uno, A Raspberry Pi 3B+ is used as a vision system of this module, which carries several video streams directly to the switch. Three USB cameras are connected with the Pi for a) Capturing the image data of rock sample, b) Monitoring the soil collection and storing process and c) Observing the output colour of the evaluation tests. The resolution of the cameras was selected keeping the contrasting characteristics such as the quality of the image and response time in consideration. For example, an HD camera with 1980×1280 resolution is fitted on top of the secondary manipulator to capture the image of the rock sample. This image is fed into Jetson NX through the switch by the Raspberry Pi, and is used as an input to the pre-trained models running in the Jetson NX. However, the feedback of the remaining two cameras were fixed at a lower resolution for transmitting to the Base-station with a faster response time.

Reliable power supply, minimization of power consumption, and maximization of cost-efficiency was considered during the design phase of the power subsystem. According
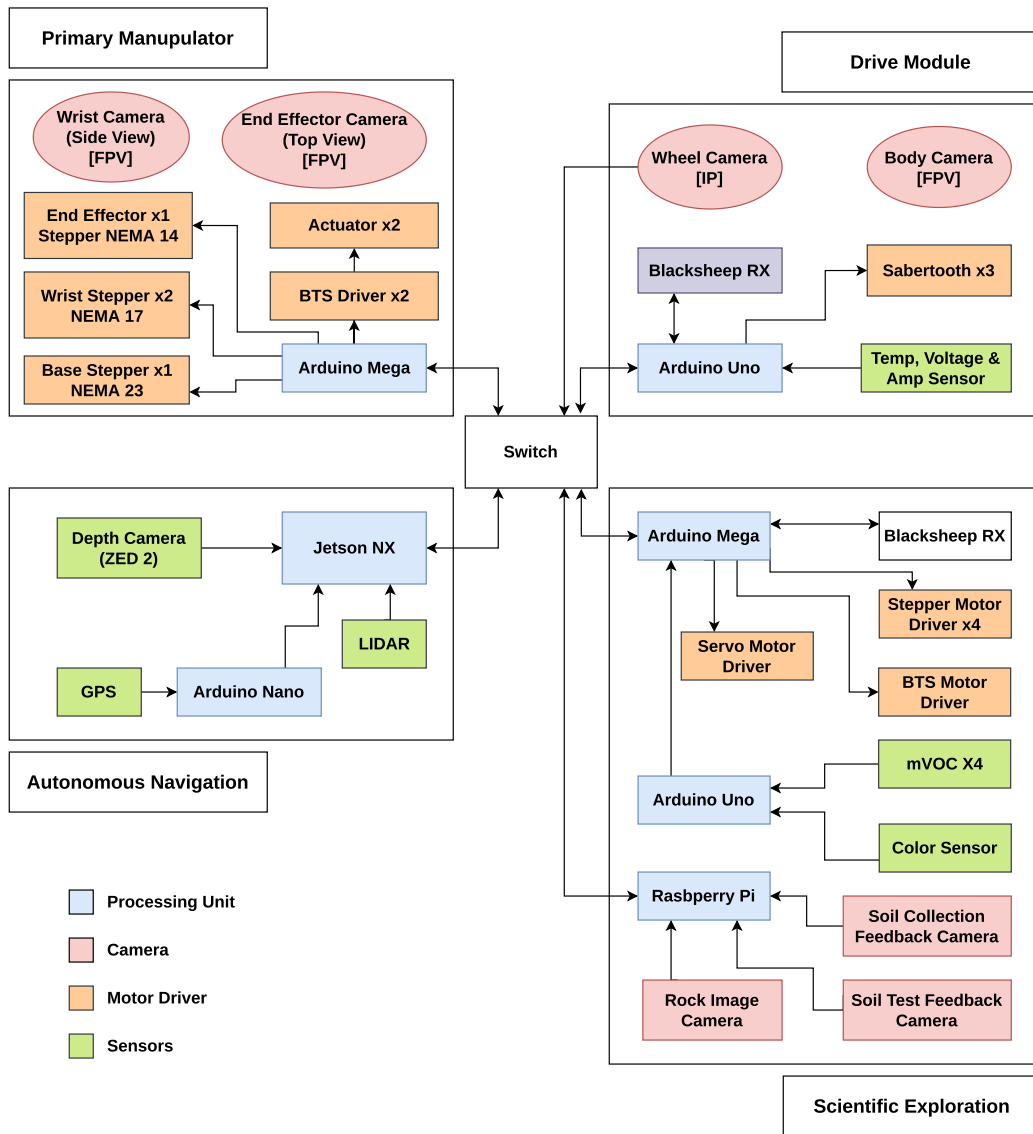
FIGURE 12. System architecture of the PHOENIX.

to the measured power consumption rate of the components used and the mission-specific requirement of a maximum of 60 minutes battery backup, 720 watts were required to be supplied (see Appendix A). The subsystem is developed into two modules; (a) 12v and (b) 24v. Lithium-polymer (Li-po) batteries are used due to their fast charging and discharging characteristics. Six 12V Li-po batteries and two 24V Li-po batteries are connected in parallel to create the 12V and 24V power modules respectively. The developed power subsystem is capable of generating 820 watts. After being fully charged, the system can provide a minimum battery backup of 70 minutes. Step down voltage regulators (XL4016 Step Down Buck) are used to supply the required amount of voltage to the components. Moreover, voltage and current indicators are used to measure their value in real-time.

V. ROVER COMMUNICATION AND CONTROL
The communication architecture (see Figure 13) of the rover is designed using a hybrid of 5 GHz, 900 MHz and 2.4 GHz bandwidths for faster and reliable communication between the rover and the base station. The higher bandwidth of 5 GHz ensures the transfer of data with reduced latency [26]. Thus, it is used for FPV cameras attached to the rover body to obtain visual feedback and transmit it to the base station. The receiving antenna at the base station receives the visual feedback transmitted by the FPV cameras using 5 GHz bandwidth. By contrast, The 900MHz band can transmit data with lower latency over a longer distance and has less possibility of interference [26]. The commands for the manual navigation of the rover, control of the primary manipulator and control of the scientific exploration subsystem require
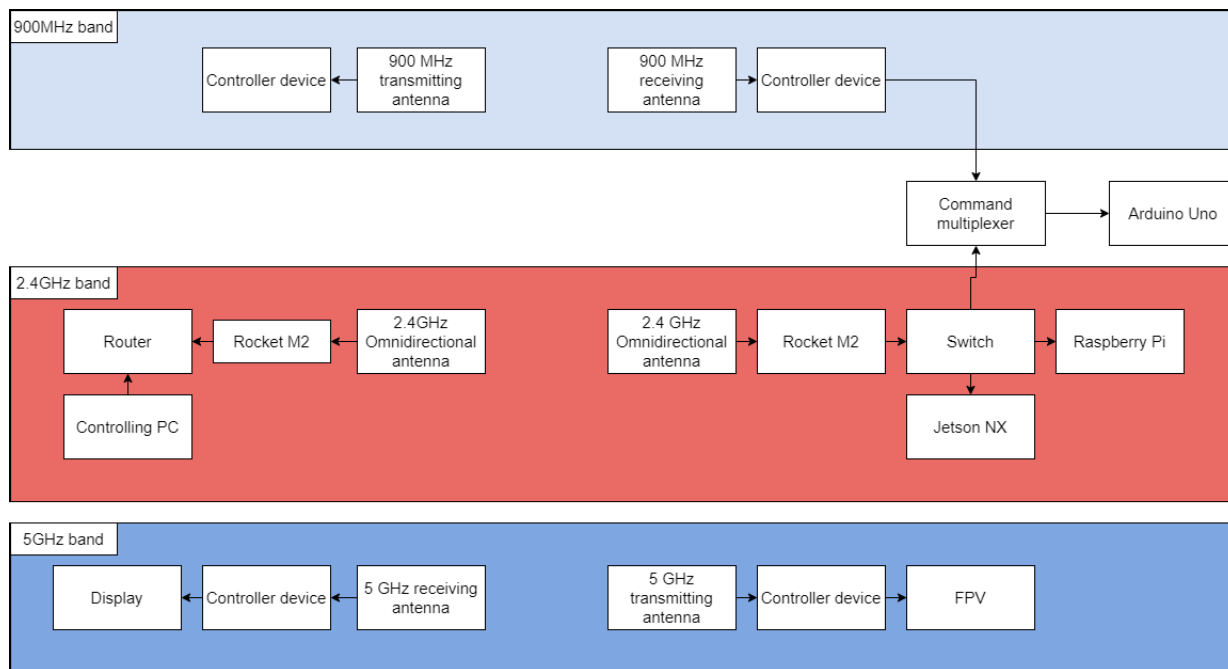
**FIGURE 13.** Control and communication architecture of the rover.

real-time transmission. As shown in Figure 13, 900 MHz Transmitter (TBS Crossfire Micro Tx) is connected with the remote controller (Radiomaster TX16S) to transmit the commands for the manual navigation from the base station. Three separate receivers (TBS Crossfire Micro Rx) connected with the processing unit of the drive, the primary manipulator and the scientific exploration subsystem responds to the transmitted commands from the base station. According to the specific mission, the remote is programmed to multiplex between the drive and primary manipulator subsystem or drive and scientific exploration subsystem. Finally, 2.4 GHz is used to transfer the sensor data from the rover to the Base station and as an alternative to command and video transmission systems. A customized multiplexer ensures the transition of commands between 2.4GHz and 900MHz bands. If any error or delay occurs in the 900MHz band, the multiplexer switches command transmission to the 2.4GHz channel. For long-distance video transmission, the conversion of each frame to grey-scale has been implemented to significantly decrease bandwidth usage and video transmission latency.

During teleoperation of the rover, operator sends direction and speed values to the rover as control signals to perform various operations including terrain traversal, equipment servicing tasks using the primary manipulator, soil sample collection using the secondary manipulator, reagent flow in the beaker of the scientific exploration subsystem, etc. However, during the autonomous navigation no control signals are sent to the rover from the base station. The rover navigates itself and the telemetry data during the navigation is recorded for further analysis. An ACK signal (along with rover status) is sent back to the Base Station as the signal feedback.

A web-based dashboard as shown in Figure 14 is developed for visualizing necessary visual feedback, sensor data, analytics from the derived data and system monitoring. A python-based Flask server running in the Raspberry Pi on the rover collects all the sensor data from the sensors of the rover. Through a periodic API call, the dashboard server collects data from the rover. Figure 14(c) highlights the visualisation of the data collected from the mVOC sensors and the input panel for the soil sample analysis. Visual feedbacks of the various orientation of the rover such as the main camera for observing the surroundings, wheel camera, primary manipulator cameras in two different angles, etc (Figure 14(b)) are live-streamed in the dashboard for situational awareness in manual navigation and equipment servicing mission. Moreover, visual feedback during the science mission such as USB microscope feedback for observing the rock sample (Figure 14(a)), camera feedback to observe the colour change in beakers during the soil sample analysis, etc. is extracted in the dashboard. Additionally, Maintenance data (Figure 14(d)) such as: battery percentage, internal system temperature, status of subsystems, etc. are also visualised in the dashboard

VI. ROVER AUTONOMOUS NAVIGATION
For navigating the rover autonomously, simultaneous localization and mapping (SLAM) algorithm is used to estimate the pose of the robot along with the development of the environmental map. The rover uses a depth-sensing camera (ZED 2) to obtain odometry and estimate its own position. zed_ros_wrapper [27] is used to access camera parameters through Robotic Operating System (ROS) topics, parameters and services and an extended Kalman
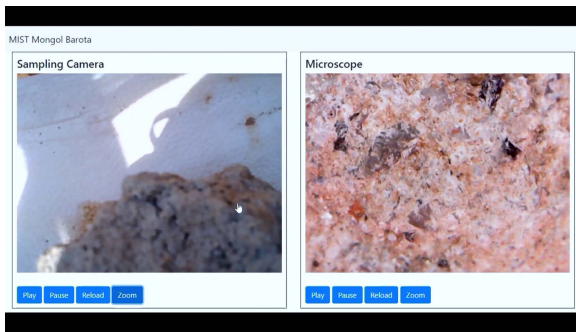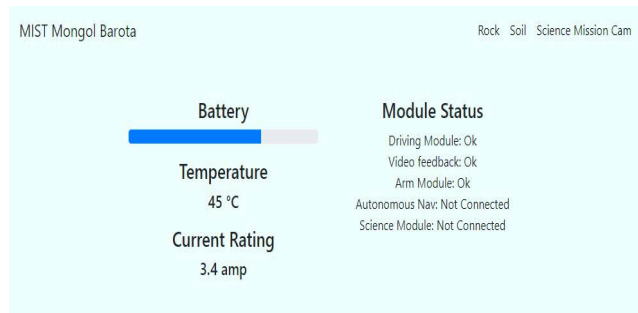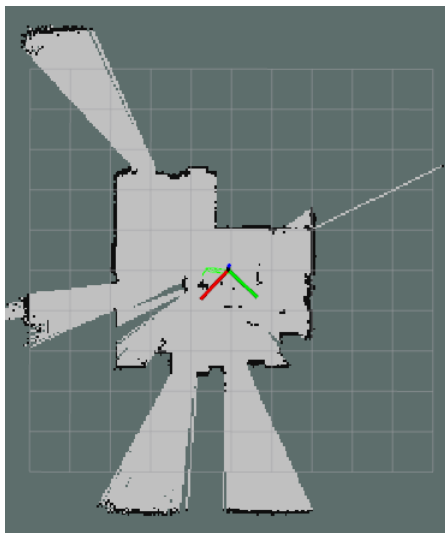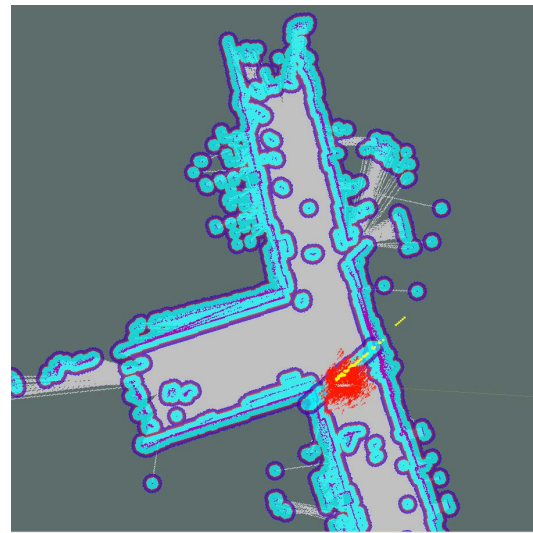
(a)
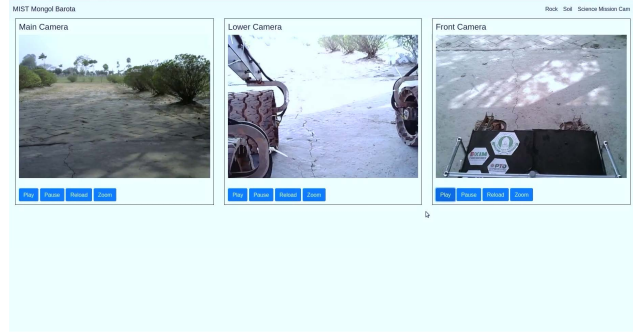
(b)
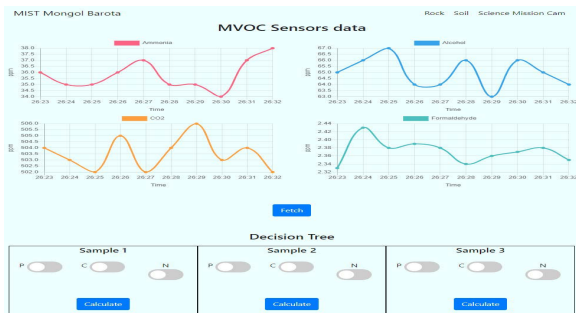
(c)

(d)

FIGURE 14. Snippets of the developed dashboard of the rover for controlling and visualisation of data.

(a)

(b)

FIGURE 15. (a) Mapping of the test area. (b) Localisation and pose estimation of the rover using SLAM.

filter algorithm is implemented using the ekf_localization node from the robot_localization [28] package to filter the obtained data. A two dimensional(2D) light detection and ranging (LIDAR) sensor (RPLIDAR A2) is adopted for mapping using rplidar_ros [29] to provide basic device handling between ROS and 2D-LIDAR; SLAM algorithm is implemented by customizing the slam_gmapping node of the gmapping [30] package which adopts Rao-Blackwellized

Particle Filter (RBPF) to build a 2D grid map that includes sensor data from LIDAR sensor and odometry from the depth-sensing camera. After generating the 2D grid map, the amcl [31] package is integrated as a probabilistic localization system for a robot moving in 2D space with the implementation of a global and local path planner (See Figure 15). The global path planner is developed using the A* algorithm and the local path planner is developed using a Dynamic Window

Approach (DWA) to plan the navigation route towards a target. The global path planner plans the path towards the target and the local path planner generates the situational prompt path through detection and avoidance of obstacles in the proposed path of the global planner. The move_base [32] package is linked with the 2D grid map to navigate the rover in the proposed path. GPS module (BN-880) is used to fetch the global positional data. This module is connected to a separate Arduino, which works as a pass-through. Data is collected from the module using the nmea_navsat_driver [33] package that provides a ROS interface for GPS devices to generate compatible NMEA sentences. This positional data is filtered by using the ekf_localization node from the robot_localization [28] package. After that, the filtered data is distributed to a ROS-based visualization tool named mapviz [34] for visualizing the area map. The GPS coordinates, i.e. targets of the rover, are converted from GPS coordinates into ROS frame coordinates using gps_goal [35] ROS package and passed to the Navigation Stack to obtain as a target.

However, GPS coordinates of a few targets were provided 5-10 meters apart from the actual point and the actual point is being marked by an Augmented Reality (AR) tag. Additionally, the competition challenges the rovers with a task to detect gates created by two AR Tags and traverse through the gates. To accommodate this requirement, AR-tag detection capability is developed using the depth-sensing camera with the integration of ar_track_alvar [36] package as shown in Figure 16. The depth data of the camera is utilized to identify and track the pose of an individual AR-tag or "bundles" consisting of multiple tags and their relative distances from the rover. In the case of gates consisting of two AR-tags, the mean point of the Euclidean distance between two nearby AR tags was calculated, before being passed to the rover as a target point.

Firstly, a customized python script loads the GPS information of all the targets as an ArrayList to the system while the rover is located at the start position on the ground and continues to run until the list is empty. The two phases of reaching from a target to another target are autonomously controlled by the rover using a flag toggle mechanism as shown in Figure 17. Initially at the start point, the flag is set to a value of 0. After reaching the GPS coordinate given for a target, the flag is switched to 1 and the navigation scheme to reach the position indicated by the AR-tag or the mean point of the distance between two tags (in the case of a gate) is being initiated by the rover. The rover drives itself using a carrot navigation technique by calculating the difference between the matrix of pose estimation and target. After reaching the target, the flag is reset to 0 and the ArrayList is updated to point towards the GPS information of the next target. A green Light Emitting Diode (LED) mounted on the rover body blinks to indicate that the rover has successfully arrived at the target and is switching to the next goal. Additionally, LEDs are mounted on the rover body to indicate whether the rover is in autonomous navigation mode (Red), or an operator has
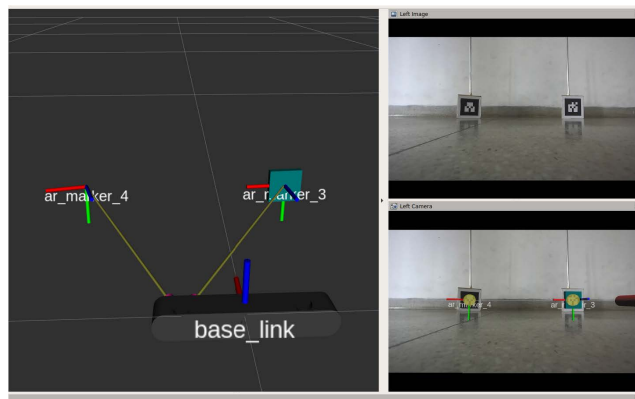

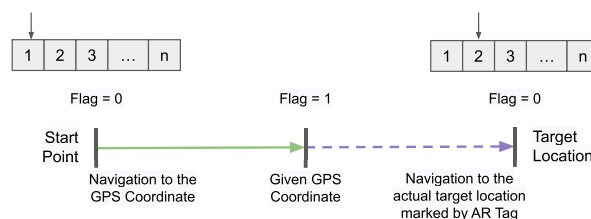**FIGURE 16.** AR Tag detection using as_track_alvar.

FIGURE 17. Autonomous navigation scheme of PHOENIX.

assumed manual control (Blue). In the event of manual control, the commands received from the operator receive priority over the autonomous navigation commands. To implement this multiplexing of control commands, cmd_vel_mux [37] package is customized to integrate with the rover's existing control systems.

VII. SCIENTIFIC EXPLORATION

Scientific exploration subsystem is developed to detect life from soil and rock samples intending to label them into three distinct categories as follws:

1) *Extant:* Life that is metabolizing or has so recently died that the biomolecules are yet to be degraded
2) *Extinct:* Life that is fossilized and no longer metabolizing
3) *No Presence of Life (NPL):* inanimate/abiotic objects [38].

A. SOIL SAMPLE

A novel architecture of rapid multiple biomolecules based life detection protocol (MBLDP-R) from soil samples is developed to detect the presence of life from the soil samples. The sample collection mechanism is discussed in the Rover Mechanics section and highlighted in Figure 11(a) and 11(b). After collecting the samples from any location, the sample is deposited into three isolated beakers for the detection of biomolecules for on-board analysis which involves: a) Detection of Carbohydrate using *Benedict's* solution, b) Detection of Protein using *Ninhydrin* solution and c) Detection of Ammonium ion using *Litmus-strip* test.
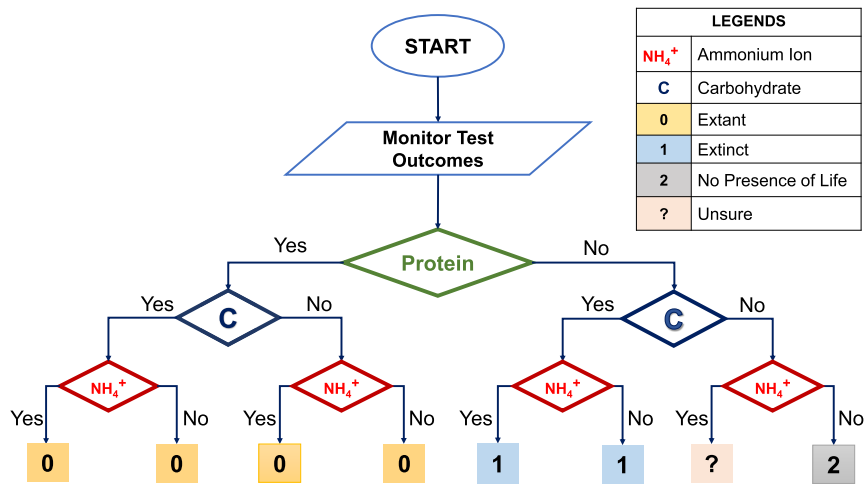
FIGURE 18. Rapid multiple biomolecules based life detection protocol (MBLDP-R) for soil sample analysis.

Figure 18 shows the architecture of the MBLDP-R for the detection of life in soil samples. Extracted information of the selected biomolecules is utilized to create the structure of the proposed protocol. In the three-layered decision-tree based architecture of the protocol, the presence of protein is checked in the first layer followed by the carbohydrate and lastly ammonium ion. There are eight possible outcomes of the proposed protocol as shown in Figure 18. The presence of all three types of biomolecules is classified as *Extant* and the absence of all three types gives a result of *NPL*. Proteins are found in all living organisms and are not found abiotically. Moreover, protein is also a notable type of biomolecule that can be found in fossils buried underground [39]. On a similar note, carbohydrates can be found in the soil samples because of microorganisms, plant tissue or tree roots-roots [40]. Carbohydrates can also be found on fossil samples belonging to specimens of protozoa, mollusca, arthropoda and plants [41]. Moreover, ancient sedimentary rocks are also a source of carbohydrates [42]. Although both proteins and carbohydrates can be found as fossil molecules, in terms of decay resistance carbohydrate is ahead of protein which indicates that the possibility of carbohydrate preservation in fossil records or incorporation into fossil fuels is more than protein [43]. For this reason, regardless of the other two types of molecules, the presence of protein will always give us a result of *Extant*. When protein is absent, the framework will prioritize on the presence of carbohydrate. If carbohydrate is present despite the absence of protein, the framework will always give a result of 'Extinct', regardless of the presence of ammonium ion (NH4+). Although ammonium ion (NH4+) can be present in living organisms, it can be produced abiotically or biotically. For this reason, only the presence of ammonium ion cannot specifically indicate any of the three results (*Extant*, *Extinct* and *NPL*). To avoid complications, this uncertain result is considered as *NPL* by the framework.

B. ROCK SAMPLE

Contamination of rock samples i.e. physical contact or deformation is not allowed. Thus, a contamination-less mechanism based on the infusion of information from the sensor data and machine learning (ML) model-based prediction is taken into consideration. Figure 20 shows the workflow of the developed framework. The major steps of the workflow are as follows:

1) PHASE 01: IDENTIFICATION OF LIVING ORGANISM ON THE SURFACE OF ROCK SAMPLE

Firstly, A USB microscope with the addition of micro volatile organic compounds (mVOC) sensors (C_2H_5OH, CH_2O, CO_2, NH_4^+), colour sensor and camera with 1980×1080 resolution is mounted on the end-effector of the secondary manipulator as shown in Figure 11(d). To check whether or not there are signs of the existence of living organisms on a given rock specimen, the USB microscope is positioned on the rock, and consequently, a visual is obtained by moving the secondary manipulator horizontally and vertically. The image thus obtained is then transferred to the dashboard, via a microprocessor (Raspberry pi 3B+) for visualisation and analysis. At the same time, mVOC sensors located around the USB microscope detect the presence of mVOC and concentrations of the compounds in the specimen. If the obtained specimen contains both visuals of living organisms on the surface of the rock and the presence of mVOC signatures the sample is labelled as *Extant*.

2) PHASE 02: DEVELOPMENT OF ML MODELS

We use the transfer learning concept to address the limitations of having a small dataset to train the CNN models. Additionally, Multi-Class Classification is replaced with the pipeline of binary classifiers to reduce the computational complexity in the main processing unit (NVIDIA Jetson NX) of the rover
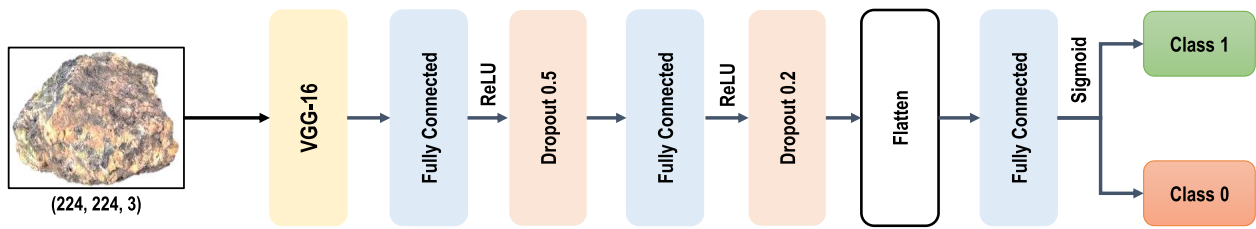
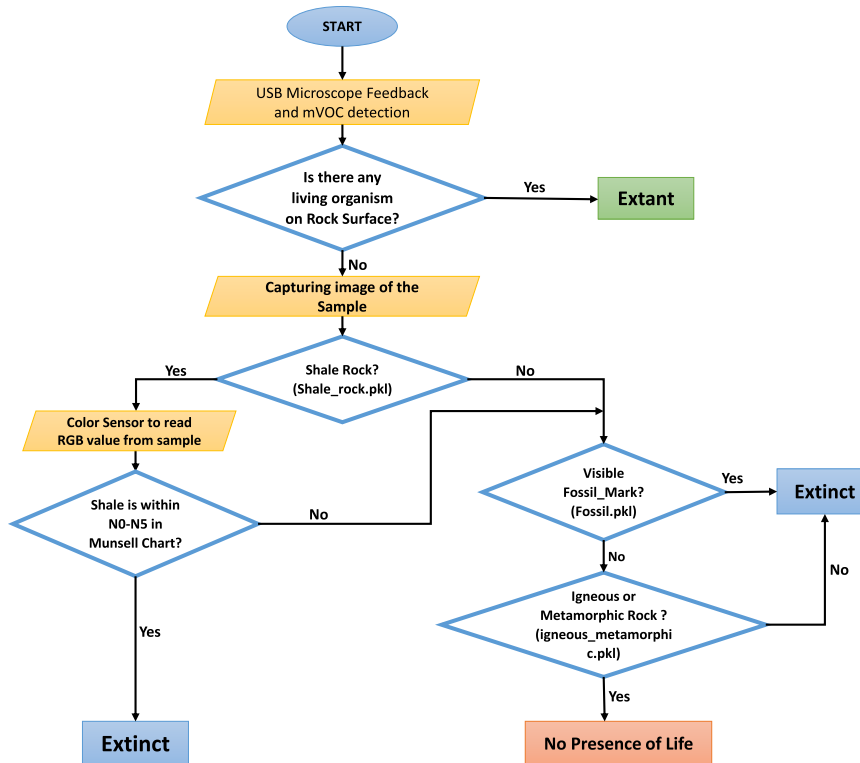**FIGURE 19. Architecture of the model in rock detection.**

FIGURE 20. DNN based Life Detection protocol for detection of life in Rock sample.

body. The outcomes of the classifiers are used in different stages of the detection of life from rock samples as shown in Figure 20.

A convolutional neural network(CNN) model is developed using the concept of transfer learning. VGG-16 is used which is a 16 layer deep CNN model trained on over 14 million high-resolution images of the ImageNet dataset and is capable to classify 1000 different objects [44]. VGG-16 pre-trained model layers are used to extract aggregated information from the input image sample of shape (224, 224, 3). Three fully connected (FC) layers are then applied to make use of the extracted information. The first two layers of 256 and 128 neurons respectively are followed by a Rectified Linear Unit (ReLU) [45] activation function as it aims to avoid exploding gradients which makes the computations faster and easier to converge. Since FC layers are likely to excessively co-adapting themselves causing overfitting, dropout is applied after each of these layers to reduce

overfitting. A flatten layer is then applied to convert the multi-dimensional data into a one-dimensional array to channel it into the final FC layer. The final FC layer of 1 neuron is followed by a smoothing sigmoid activation function [46] and the prediction result is obtained from this layer.

A total of 486 image samples are collected comprised of shale, limestone, conglomerate, sandstone, metamorphic and igneous rocks. 178 samples out of 486 are rock samples with fossil marks. Three separate binary classifiers are developed using the architecture as shown in Figure 19 and trained separately on the following dataset:

- Shale Classifier: We use 286 samples (132 Shale and 154 Non-Shale) to construct the model and save the model as shale.pkl.
- Igneous-Metamorphic Classifier: We use 386 samples (189 Igneous-Metamorphic and 197 Non-Igneous-Metamorphic) to construct the model and save the model as igneous_metamorphic.pkl.

TABLE 1. Performance metrics of the developed classifier models on test dataset.

Models	ACC	PR	R	F1
Shale Classifier	95.89	94.65	92.71	93.67
Igneous-Metamorphic Classifier	94.54	93.43	90.82	92.11
Fossil Classifier	98.07	97.29	95.78	96.53

- Fossil Classifier: We use 367 samples (178 Fossilized and 189 Non-Fossilized) to construct the model and save the model as fossil.pkl.

We choose Adam [47] as the optimizer due to its good learning rate and parameter specific adaptive nature of the learning rates. The initial learning rate is set as 0.003. Binary Cross-entropy is used as the loss function to derive the closeness between predicted and actual distributions. The batch size is set to 16 and each of the models is trained for 20 epochs. For every model, a ten-fold cross validation is conducted by dividing the samples into 10 groups. For each round, we select one group of samples as testing data and the remaining 9 groups as training data. Finally, we combine the predicted class from all the 10 rounds to calculate the performance metrics. We adopt four metrics: accuracy (ACC), precision (PR), recall (R) and F1-score (F1) to evaluate the performance of the models for classification. Table 1 highlights the performance metrics of the developed models on the testing dataset. All three models show a F1-score of more than 90% with Fossil classifier demonstrating the highest performance with a score of 96.53% and Igneous-Metamorphic classifier demonstrating the highest performance with a score of 92.11%.

3) PHASE 03: DETECTION OF SHALE ROCK
Camera mounted on the secondary manipulator (see Figure 11(d)) captures the image of the rock sample which is fed into the Jetson NX processor for necessary preprocessing. The preprocessed image is fed as an input into the trained model ''shale.pkl'' to predict the sample into *shale* or *not_shale* class. In parallel, a reading is taken from the colour sensor and a comparative analysis with the Munsell rock colour chart is used to label the sample ranging from N0 to N9 [48]. The reading between N0 to N5 in the Munsell rock colour chart depicts the presence of high Total Organic Carbon (TOC). If the rock is predicted as *shale* and the reading from the colour sensor is between N0 to N5 the sample is labelled as *Extinct*. If the rock is predicted as *not_shale* or the reading from the colour sensor is not within the desired range, phase 03 is being initiated.

4) PHASE 04: DETECTION OF FOSSIL MARK
The preprocessed image is used as an input to the pretrained model ''fossil.pkl'' to classify the sample into either *fossilized*

or *not_fossilized*. Being classified as *fossilized* the sample is labelled as *Extinct*. Results on the contrary initiates the Phase 04.

5) PHASE 05: DETECTION OF THE IGNEOUS OR METAMORPHIC ROCK
Similar to Phase 2 and 3, the image is used as an input to the pre-trained model ''igneous_metamorphic.pkl'' to classify the sample into either *igneous_metamorphic* or *not_igneous_metamorphic*. Igneous and Metamorphic rocks do not contain any presence of life and also the fossils are being cluttered during the transformation process from sedimentary rocks [49]. Thus, If the rock sample is classified as igneous or metamorphic, it is labelled as *NPL*. If the rock is not igneous or metamorphic the sample is classified as *Extinct*.

VIII. EVALUATION OF FEATURES
The rover is evaluated into two broad categories: a) General capability evaluation and b) Mission oriented capability evaluation. The evaluation study is conducted in mock competition environments created in the authors' institute. Most of the capabilities are also demonstrated successfully during the actual competition.

A. GENERAL CAPABILITY EVALUATION
Evaluation of the general capabilities of the rover is conducted to find out the degree of precision of the basic movements (straight traversal, rotation capability) and feedback of the communication system. Various terrains (concrete, sandy, grass) are used to conduct evaluation on (chassis + primary manipulator) and (chassis + scientific exploration) configuration. The rover successfully complete all of the tests as highlighted in Table 2.

B. MISSION-ORIENTED TESTS
1) TERRAIN TRAVERSAL TEST
The rover is developed to traverse various types of Mars-like terrains such as rock and boulder fields, soft sandy areas, rough stony regions etc. In the Terrain Traversal test, the capability of the rover to traverse these places are observed and the result of the tests are documented in Table 3. The rover could successfully climb a slope of a minimum of 15° and a maximum of 30° in different types of terrain. Additionally, a vertical drop of 1 meter is tested to observe the shock absorption capability of the rover and to achieve competition readiness. However, the rover fails to perform the task. To analyze the limitations, a Drop test simulation is performed on the rover in SolidWorks. The material condition is set to linear and the contact condition between the shaft and rocker to non-penetrating condition. The maximum stress obtained is 650Mpa, which is more than the elastic limit of the material (stainless steel) used. The simulation is done from progressively increasing height starting from 0.1m and incremented by 0.1m each time. At 0.5m height, it is observed

TABLE 2. Summary of the general capability evaluation study.

Test Type	Configuration	Terrain	Status
10-meter Straight traversal	With Primary Manipulator	Concrete	Success
		Sandy	Success
		Grass	Success
	Science Exploration Subsystem	Concrete	Success
		Sandy	Success
		Grass	Success
Rotation (clockwise and anti-clockwise)	With Primary Manipulator	Concrete	Success
		Sandy	Success
		Grass	Success
	Science Exploration Subsystem	Concrete	Success
		Sandy	Success
		Grass	Success
A 50-meter route containing straight and rotation movement	With Primary Manipulator	Concrete	Success
		Sandy	Success
		Grass	Success
	Science Exploration Subsystem.	Concrete	Success
		Sandy	Success
		Grass	Success

from the simulation that the rover sustains a permanent wheel joint deformation. This happens because the suspension of the tire of the wheels is a rigid system which is installed with the sole purpose of providing stability, not to absorb the sudden shock and vibration. Thus, the rover is reevaluated with a vertical drop of 0.5 meters. The test is successful in each of the three attempts this time (see Table 3). The rover demonstrates the 30° slope traversal in the competition day and bypassed the 1-meter vertical drop challenge.[1]

2) SCIENTIFIC EXPLORATION
An evaluation study is conducted in the mock science mission ground of the authors' institute to evaluate the scientific exploration capability i.e. detection of life from soil and rock samples. A mock set-up of URC 2021 is prepared with 7 samples (4 soil and 3 rock) at a time. At first, the samples are placed in their designated area and the tasks are assigned to the controller to complete all of the tasks within 40 minutes. The distance between each sample is set randomly around the experiment field and The ground condition is sandy. This test is repeated 10 times for evaluating the performance of the rover. Thus, through the evaluation study, 40 soil samples (18 *Extant*, 12 *Extinct* and 10 *NPL*) and 30 rock samples (15 *Extant*, 14 *Extinct* and 11 *NPL*) are evaluated during the 10 mock cases.

The soil samples are collected from a local site. However, the necessary alteration is implemented to increase the bioload or remove it. According to the guidelines of URC 2021, the samples are labelled as Extant, Extinct and No Presence of Life (NPL). The Extant samples are prepared by collecting fertile soil and removing any unwanted rock particles. A few of the samples are modified using extra bioloads (dextrose, albumin, etc.). The No Presence of Life (NPL) samples are prepared by baking the soil for more than 24 hours at 500 degrees centigrade according to the exact guideline of the URC organizing committee [50]. The Extinct samples are

[1]https://www.youtube.com/watch?v=dycsxAs_nGQ

prepared in two phases. In phase one, the collected samples are baked for more than 24 hours at 500 degrees centigrade to degrade any type of presence of biosignatures. Then in phase two, fossilized rocks collected from archaeologically significant local sites are crushed and mixed with the samples to create an Extinct status

The study reveals that the life detection protocol for the soil samples, MBLDP-R is 90% (36 out of 40) accurate in classifying the samples into desired labels. The experimental data is available in Appendix A. In the case of *Extant* samples, the protocol achieves an accuracy of 94.44% (17 out of 18). For *Extinct* and *NPL* samples the protocol is found to be 83.33% (10 out of 12) and 90% (9 out of 10) accurate respectively. Among the three classes, *Extant* samples are better predicted by the protocol with an F-score of 97.14, followed by *NPL* class with a score of 85.71 and lastly *Extinct* Class with a score of 83.33. In the proposed protocol, the micro average for recall, precision and F-score is 89.25, 88.38, and 88.72 respectively. This is a single labelled multi-classification problem therefore in the case of micro average, both the precision and recall are equal to the accuracy of the protocol i.e., 90% which deduced the harmonic mean i.e. micro F1 score as 90. Additionally, area under the Receiver Operating curve (AUC-ROC) is 0.92 (See Figure 21) which depicts that 92% of the test cases are correctly predicted. Moreover, the *Extant* class (0.97) is the highest with *NPL* (0.92) and *Extinct* (0.88) follows with a little margin among themselves. The average time required for the completion of the tests is 17.6 minutes while the minimum time is 15.20 minutes and the maximum time is 19.45 minutes. For *Extant* samples, the time is 17.3 minutes, for *Extinct* it is 16.8 minutes and for *NPL* it is 18.2 minutes. Moreover, negative tests take a little longer with an average of 18.4 minutes. All three-Positive tests took the least time for completion, with an average of 15.2 minutes.

The rock samples are prepared using various types of rocks (limestone, conglomerate, sandstone, granite, basalt, marble). Extant samples were prepared by placing algae

TABLE 3. Terrain Traversal Test.

Test type	Configuration	Terrain	Status
Slope traversal (min 15° to max 30°)	With Primary Manipulator Science Exploration Subsystem.	Rock, Sandy Rock, Sandy	Success Success
Vertical Drop of 1 meter	With Primary Manipulator	Sandy	Failure
Vertical Drop of 0.5 meter	With Primary Manipulator	Sandy	Success

TABLE 4. Autonomous Navigation Test.

| Test type	Objective	Experiment Setup	Status
Test 01: AR-tag detection	Detect an AR-tag or Multiple AR-tags successfully	Open Field, Grass, Mock Set-Up similar to the competition	Success
Test 02: GPS test	Finding out the accuracy of the data of GPS sensor	Open Field, Grass, Mock Set-Up similar to the competition	Success; accurate with a mean error of 1.53 ± 0.45 meters
Test 03: Navigation Test	Determine the capability of traversal to a predefined target	Open Field, Grass, Mock Set-Up similar to the competition	Success; accurate with a mean error of 0.673 ± 0.42 meters
Test 04: Overall autonomous navigation evaluation	Finding out the performance of the developed navigation subsystem	Open Field, Grass, Mock Set-Up similar to the competition	Success
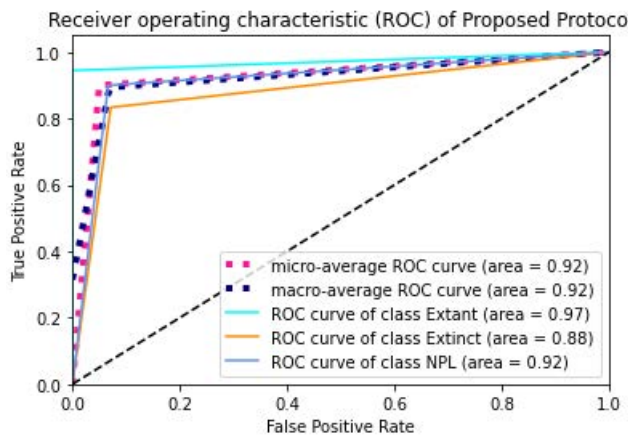
FIGURE 21. AUC-ROC of MBLDP-R for soil sample analysis.

(*Ascophyllum nodosum*) strip on top of 12 of the 30 rock samples. Additionally, 8 Fossiliferous Limestones are taken as the Extinct samples and the rest of the rocks were taken as No Presence of Life Samples. 28 out of 30 samples are correctly predicted by the developed protocol. The experimental data is available in Appendix B. The protocol shows an average accuracy of 93.33% with the successful detection of 11 out of 12 (91.67%) Extant samples, 7 out of 8 (87.5%) Extinct samples and 10 out of 10 (100%) NPL samples. Additionally, the protocol achieve this success without the addition of any element analysis tool (Raman Spectrometer or X-ray fluorescence) which enables the protocol to be cost-effective yet functional with similar amount of accuracy.

3) HUMAN ASSISTANCE (DELIVERY AND RETRIEVAL)
Following three tasks are conducted several times during the preparation phase and are also successfully demonstrated on the competition.[2] **Test 01**: Lift 5.5 kg using the primary manipulator and deliver it to a definite position for human assistance. Status: *Success* **Test 02**: Grab a rope (minimum 6 mm diameter) that contains a maximum of 4 kg at the other end and drag it up to 2.5 meters. Status: *Success* **Test 03**: Grab a screwdriver (at least 15 cm) from the ground and precisely deliver it in a 30 cm×30 cm marked area on the ground. Status: *Success*

4) EQUIPMENT SERVICING TEST
Equipment Servicing tasks are evaluated using a mock spaceship with 4-sided panels. For better preparation for the competition, the following tests were conducted setting up an actual competition environment several times before the competition and are also demonstrated successfully on the final day of the competition[3] by achieving a perfect 100 out of 100 in the Equipment Servicing Mission: **Test 01:** Open a drawer, Insert a toolbox in the drawer and close it (Maximum weight of the toolbox 3.5 kg.). Status: *Success*; **Test 02:** Type a 3-letter code on the keyboard. Status: *Success*. **Test 03:** Pick up a USB memory stick and insert it into a USB (Type A) slot. Status: *Success*. **Test 04:** Flip three toggle switches to turn on the power. Status: *Success*. **Test 05:** Tighten a head screw (8 mm and 12 mm Allen Hex). Status: *Success*. **Test 06:** Use a joystick to move a gauge for setting up a specific voltage in the voltmeter. Status: *Success*.

[2]https://www.youtube.com/watch?v=dycsxAs_nGQ
[3]https://youtu.be/gQDG76S0j-E

5) TELEOPERATION TEST

All of the tasks of delivery and equipment servicing mission are conducted using manual control or teleoperation. To exclusively evaluate the teleoperation of the robot, several sets of operations are accumulated to design a case study where the operator controlled the robot using the remote control or teleoperation. Following operations are completed sequentially by the robot in this case study:

- Traverse to Start Point to Point-01 (800 m)
- Pick up a box of 5 kg at Point-01
- Traverse from Point-01 to Point-02 and deliver the box. (300 m)
- Rotate the knob switch to switch on the main power of a mock lander at Point-02
- Traverse from Point-02 to Point-03 (300 m)
- Pick up a Water Can and use it to water the plant at Point-03
- Carry the Water Can to the End Point (100 m)

The responsiveness of the robot in case of command transmission and follow-up action time is measured during several iterations of this case study. The average response time to transmit a command and the robot to respond is found to be approximately 0.034 seconds where the robot is within 500 metres to the control station and 0.121 seconds where the robot is more than 1000 metres away from the control station. The operators are able to complete the case study performing all the operations sequentially. The avearge time of completion of the case study is 19 miuntes 25 seconds (trialed 16 times by two operators of the team)

6) AUTONOMOUS NAVIGATION TEST

An autonomous navigation test is conducted with and without the primary manipulator. In a similar type of mock set-up of URC, an open grassy field is selected for the study. The test is conducted in four phases (See Table 4): a) Detection of AR-tag b) Accuracy of obtained GPS feedback and c) Path planning capability and d) integration and regression test of the full subsystem.

IX. DISCUSSION AND CONCLUSION
A. PRINCIPAL RESULTS

In this study, a modular human assistant rover with planetary exploration capabilities is developed. Structural analysis is conducted on the mechanical design of the rover to analyse stress and deformation. To increase the performance of the primary manipulator, a semi-differential mechanism through three bevel gears with two DOF is introduced in its wrist. A hybrid communication subsystem using 900 MHz, 2.4 GHz and 5 GHz is used to ensure the required range of 2-3 km uninterrupted non line of sight communication for command transfer and video transmission from the rover. A detailed evaluation of the developed robotic system demonstrates the design validity of the rover. Along with the general capability of the rover, the mission-oriented capabilities are also successfully evaluated during the mock tests and the competition

day. A successful result in the terrain traversal test in various terrains shows the manoeuvring capability of the rover and signifies the well-designed constructed chassis subsystem of the body. It also indicates the successful integration of the other subsystems (science exploration and primary manipulator) in the rover system. The developed autonomous navigation subsystem is successful to drive the robot autonomously from one point to another avoiding obstacles in the route using the developed algorithm. Moreover, the novel scientific exploration subsystem is successfully tested to detect the presence of life from soil and rock samples by classifying the samples into *Extant*, *Extinct*, and *NPL*. A high recall (89.25), precision (88.38) and F1-Score (88.72) of the developed Multiple biomolecules based soil detection protocol (MBLDP-R) along with an acceptable AUC value (0.92 Micro and 0.97 Macro) from the evaluation study indicate the effectiveness and reliability of this protocol to detect signatures of life from soil samples. Moreover, an average time of 17.6 minutes for completing a full detection ensure that the requirement of the protocol to be rapid is met. Additionally, 28 out of 30 rock samples during the mock test are accurately detected with the developed protocol for life detection in rock samples. The protocol show an average accuracy of 93.33% with the successful detection of 11 out of 12 (91.67%) *Extant* samples, 7 out of 8 (87.5%) *Extinct* samples and 10 out of 10 (100%) *NPL* samples. Additionally, the protocol achieves this accuracy without the help of any costly element analysis tool (Raman Spectrometer or X-ray fluorescence) thus proving itself cost-effective with similar accuracy. The rover is also capable of performing sophisticated tasks like typing in the keyboard, inserting a USB memory stick into a slot, setting up a reading using a joystick controller, grabbing a screwdriver, opening an allen hex screw, etc. These capabilities are expected to be useful for assisting an astronaut in planetary exploration in risky environment.

B. COMPARISON WITH PRIOR WORKS

Unlike few of the prior works [22], [23], PHOENIX is equipped with an autonomous navigation system which is capable of path planning towards a set of GPS location defined goals that are marked by AR-tag and can avoid the obstacles en route. Most of the previous works [23], [24] highlighted the collection of sample capability and developed a soil habitability testing subsystem. PHOENIX has incorporated these works, and extended upon the functionalities to develop a unique scientific exploration subsystem capable of on-board life detection from both rock and soil samples. In addition, the soil samples can be collected comprehensively and measures are taken to avoid cross contamination unlike the prior works [23], [24].

The findings of the evaluation study of the scientific exploration subsystem shows that the developed life detection protocol MBLDP-R is effective in detecting the bio-signatures in soil samples and classify them into three desired classes as Extant, Extinct and No Presence of Life (NPL). In contrast to prior works where a single biomolecule-based detection

TABLE 5. Evaluation Data of Soil Samples using the developed MBLDP-R protocol.

Event No	Sample No	Protein	Ammonium	Carbohydrate	Predicted Label	Actual Label	Time Elapsed
1	1	Yes	No	Yes	Extant	Extant	16.45 min
	2	Yes	Yes	Yes	Extant	Extant	15.35 min
	3	No	No	No	NPL	NPL	17 min
	4	No	No	Yes	Extinct	Extinct	15.45 min
2	1	Yes	No	Yes	Extant	Extant	16.15 min
	2	No	No	No	NPL	NPL	17.45 min
	3	Yes	Yes	Yes	Extant	Extant	16 min
	4	No	Yes	Yes	Extinct	Extinct	15.40 min
3	1	Yes	No	No	Extant	Extant	17.20 min
	2	No	No	Yes	Extinct	Extinct	15.20 min
	3	No	Yes	No	NPL	NPL*	19.45 min
	4	Yes	Yes	Yes	Extant	Extant	16.10 min
4	1	No	Yes	No	Extinct	NPL*	16.10 min
	2	Yes	No	Yes	Extant	Extant	16.55 min
	3	No	Yes	Yes	NPL	Extinct	15.10 min
	4	No	No	No	NPL	NPL	18.45 min
5	1	Yes	No	Yes	Extant	Extant	16.45 min
	2	No	No	Yes	Extinct	Extinct	18.10 min
	3	No	No	No	NPL	NPL	16.30 min
	4	Yes	No	No	Extinct	Extant	18 min
6	1	No	No	No	NPL	NPL	19.04 min
	2	Yes	Yes	Yes	Extant	Extant	16.05 min
	3	No	Yes	No	NPL	NPL*	19 min
	4	Yes	Yes	Yes	Extant	Extant	15.45 min
7	1	No	Yes	Yes	Extinct	Extinct	16.13 min
	2	No	No	No	NPL	NPL	18.30 min
	3	Yes	Yes	Yes	Extant	Extant	16.15 min
	4	No	No	Yes	Extinct	Extinct	16.46 min
8	1	Yes	No	Yes	Extant	Extant	16.24 min
	2	No	Yes	Yes	Extinct	Extinct	17.12 min
	3	Yes	Yes	Yes	Extant	Extant	15.40 min
	4	No	No	Yes	NPL	Extinct	19.04 min
9	1	Yes	No	Yes	Extant	Extant	15.25 min
	2	No	Yes	Yes	Extinct	Extinct	16.30 min
	3	Yes	Yes	Yes	Extant	Extant	16.50 min
	4	No	No	Yes	Extinct	Extinct	16.44 min
10	1	Yes	No	Yes	Extant	Extant	15.45 min
	2	No	Yes	Yes	Extinct	Extinct	16.52 min
	3	No	No	No	NPL	NPL	18.36 min
	4	Yes	Yes	Yes	Extant	Extant	15.59 min

system [51]–[54] and theoretical framework-based contributions [55]–[57] were established, the developed MBLDP-R shows improvement in various aspects. Unlike the other protocols based on a single biomolecule, multiple integration of biomolecules decrease the possibility of getting false negatives. For example, in the case of the single biomolecule based method of Mora et. al. [53], a sample would be termed as No Presence of Life (NPL) if an amino acid is absent in that sample. However, other biomolecules, which remain unidentified due to the limitation of the structure of the protocol, cannot contribute to classify the sample. However, the developed MBLDP-R is capable of detecting life in the absence of amino acids as it utilizes the presence of both carbohydrates and ammonium ions or only carbohydrates to classify the sample as Extant. A similar statement is also true for the works [51], [52], [54] where only nucleic acid was used to detect the signature of life. On contrary, the developed MBLDP-R indicates better performance in classifying samples by considering all possible conditions regarding the presence of proteins, carbohydrates and ammonium ions unlike the previously developed life detection protocols. Additionally, the developed subsystem with the implemented

protocol is also resource and time efficient unlike some of the prior life detection protocols [51], [53], [54].

C. REUSABILITY OF ROVER FEATURES IN HUMAN ASSISTANCE (EXCEPT PLANETARY EXPLORATION)

The developed rover is not limited to only planetary exploration, but is rather intended to be of use in various situations playing an assitive role to humans. The independent subsystems, along with the system of PHOENIX as a whole, can be used in real life scenarios with minimal modifications. Moreover, along with space exploration, the different features of the rover can be useful in different humanitarian and research aspects by dint of its multifarious capabilities as follows:

1) AGRICULTURE AND SOIL RESEARCH

The science exploration subsystem is not only capable of detecting life, rather it is also capable of measuring the habitability of a place using the mVOC sensor readings. Additionally, various sensors, such as: pH, humidity, etc. can be added with the secondary manipulator for effective use in Agricultural and soil research. The readings of the sensors can drive the improvement of productivity, quality of crops by

TABLE 6. Evaluation Data of Rock Samples using the developed framework.

Event No	Sample No	Actual Label	USB Microscope	mVOC Sensor	Shale Predictor	Munsell Module	Fossil Predictor	Igeneous_ Metamorphic Predictor	Predicted Label
1	1	Extinct	N	N	Y	N5	-	-	Extinct
	2	Extant	Y	Y	-	-	-	-	Extant
	3	NPL	N	N	N	-	N	Y	NPL
2	4	Extinct	N	N	N	-	Y	-	Extinct
	5	Extant	Y	Y	-	-	-	-	Extant
	6	NPL	N	N	N	-	N	Y	NPL
3	7	Extinct	N	N	N	-	Y	-	Extinct
	8	Extinct	N	N	Y	N4	-	-	Extinct
	9	Extant	Y	N	-	-	-	-	Extant
4	10	NPL	N	N	Y	N9	N	Y	NPL
	11	Extant	Y	N	-	-	-	-	Extinct
	12	Extant	Y	Y	-	-	-	-	Extant
5	13	Extant	N	N	-	-	-	-	Extant
	14	NPL	N	N	N	-	N	Y	NPL
	15	NPL	N	N	N	-	N	Y	NPL
6	16	Extinct	N	N	N	-	N	Y	NPL
	17	Extant	Y	Y	-	-	-	-	Extant
	18	NPL	N	N	N	-	N	Y	NPL
7	19	Extinct	N	N	Y	N3	-	-	Extinct
	20	Extant	Y	Y	-	-	-	-	Extant
	21	NPL	N	N	N	-	N	Y	NPL
8	22	Extinct	N	N	N	-	Y	-	Extinct
	23	Extant	Y	Y	-	-	-	-	Extant
	24	NPL	N	N	N	-	N	Y	NPL
9	25	Extant	Y	N	-	-	-	-	Extant
	26	Extant	Y	Y	-	-	-	-	Extant
	27	NPL	N	N	N	-	N	N	NPL
10	28	Extinct	N	N	Y	N5	-	-	Extinct
	29	NPL	N	N	N	-	N	N	NPL
	30	Extant	Y	Y	-	-	-	-	Extant

their genetic improvement, better plant protection, irrigation, storage methods and better management of resources.

2) MILITARY PURPOSE

The developed rover can also be used during terrorist attacks, as an assistant to military personnel, to rescue targets and handle explosives using teleoperation or autonomous mode with minimum modification in the payload capability of the primary manipulator. The rover is capable of multiple use in case of handling explosives such as: collecting visual information of an improvised explosive device (IED) for the explosive disposal unit, removing a suspicious object to a favorable location and even disposing the explosives (modification will be required in manipulator), etc. Moreover, medical aids can be also be sent using the rover in a military operation zones that are risky for humans, as the rover is capable of travelling and running on places that are inconvenient for humans and standard-issue vehicles.

3) MEDICAL ROBOTICS

The developed five DOF primary manipulator shows promising use in medical robotics research, as it provides decent precision. Modification of the end effector is required for usage in medical robotics. Moreover, during this pandemic situation the robot can also be used in delivering sensitive products that require fragile manipulation to COVID-affected wards in a hospital without human assistance (modification in autonomous navigation required) or using manual control.

D. LIMITATIONS AND FUTURE SCOPES

Though the rover is successful in achieving the capabilities required to be a human-assistant rover in planetary exploration, there are several scopes for improvement in the rover. The primary manipulator is controlled using the forward kinematics which can be improved with the implementation of inverse kinematics which will useful for achieving higher precision. Moreover, the wheel mechanism can be improved with a self-rotating motion to increase mobility. Moreover, the modularity of the rover and unit testing of the subsystem shows a potential future scope of improving and utilising the subsystems in different real-life use-cases including soil research, military and medical robotics.

APPENDIX A
EVALUATION DATA OF LIFE DETECTION ON SOIL SAMPLES USING MBLDP-R
See Table 5.

APPENDIX B
EVALUATION DATA OF LIFE DETECTION ON ROCK SAMPLES USING DEVELOPED PROTOCOL
See Table 6.

AUTHOR CONTRIBUTIONS

Akib Zaman: Conceptualization, Methodology, Validation, Writing - Original Draft; Mohammad Shahjahan Majib: Resources, Writing - Original Draft, Supervision; Shoeb Ahmed Tanjim: Software, Writing - Original Draft; Shah Md. Ahasan Siddique: Design, Fabrication, Writing - Original Draft; Fardeen Ashraf: Investigation, Writing - Original Draft; Shafayetul Islam: Investigation, Validation; Abu Hena Md Maruf Morshed: Design, Writing - Original Draft; Shadman Tajwar Shahid: Design, Fabrication; Ishraq Hasan: Investigation, Writing- Reviewing and Editing; Oliullah Samir: Design, Fabrication; Safwan Shafquat: Design, Fabrication; Naim Ibna Khadem Al Bhuyain: Investigation, Validation; Asif Mahmud Rayhan: Fabrication; Md. Mushfik Ul Islam: Fabrication; Md. Akhtaruzzaman: Supervision, Writing- Reviewing and Editing; Md. Mahbubur Rahman: Supervision, Writing- Reviewing and Editing;

REFERENCES

[1] K. Yoshida, "Achievements in space robotics," *IEEE Robot. Autom. Mag.*, vol. 16, no. 4, pp. 20–28, Dec. 2009.

[2] I. M. da Fonseca, "Space robotics and associated space applications," in *Vibration Engineering and Technology of Machinery*. Cham, Switzerland: Springer, 2021, pp. 151–170.

[3] P. Putz, "Space robotics in Europe: A survey," *Robot. Auton. Syst.*, vol. 23, no. 1, pp. 3–16, 1998. [Online]. Available: https://www.sciencedirect.com/science/article/pii/S0921889097000535

[4] T. B. Nasir, M. A. M. Lalin, K. Niaz, M. R. Karim, and M. A. Rahman, "EEG based human assistance rover for domestic application," in *Proc. 2nd Int. Conf. Robot., Electr. Signal Process. Techn. (ICREST)*, Jan. 2021, pp. 461–466.

[5] R. Manikandan, K. Subash, T. J. Sujith, R. Jayasuriyan, J. Jerendran, T. Rajpradeesh, and S. Rajesh, "Design and development of an industrial firefighting rover," *Mater. Today*, vol. 45, pp. 7965–7969, 2021.

[6] S. Choudhury, S. Sawant, L. Bidwalkar, M. Marathe, and S. Das, "Design and implementation of autonomous rover for wildfire extinguishing," in *Proc. IEEE Int. Conf. Innov. Technol. (INOCON)*, Nov. 2020, pp. 1–6.

[7] A. G. Menon and M. Prabhakar, "Smart agriculture monitoring rover for small-scale farms in rural areas using IoT," in *Proc. Int. Conf. Innov. Comput., Intell. Commun. Smart Electr. Syst. (ICSES)*, Sep. 2021, pp. 1–10.

[8] A. Banos, J. Hayman, T. Wallace-Smith, B. Bird, B. Lennox, and T. B. Scott, "An assessment of contamination pickup on ground robotic vehicles for nuclear surveying application," *J. Radiol. Protection*, vol. 41, no. 2, p. 179, 2021.

[9] B. Bird, A. Griffiths, H. Martin, E. Codres, J. Jones, A. Stancu, B. Lennox, S. Watson, and X. Poteau, "A robot to monitor nuclear facilities: Using autonomous radiation-monitoring assistance to reduce risk and cost," *IEEE Robot. Autom. Mag.*, vol. 26, no. 1, pp. 35–43, Mar. 2019.

[10] J. Wilson, "NASA's orion flight test and the journey to Mars," NASA, Washington, DC, USA, Tech. Rep. N/A, 2015.

[11] H. Chen, T. Sarton du Jonchay, L. Hou, and K. Ho, "Integrated *in-situ* resource utilization system design and logistics for Mars exploration," *Acta Astronautica*, vol. 170, pp. 80–92, May 2020.

[12] K. Bussmann, A. Dietrich, and C. Ott, "Whole-body impedance control for a planetary rover with robotic arm: Theory, control design, and experimental validation," in *Proc. IEEE Int. Conf. Robot. Autom. (ICRA)*, May 2018, pp. 910–917.

[13] J. Kim, H. Jeong, and D. Lee, "Performance optimization of a passively articulated mobile robot by minimizing maximum required friction coefficient on rough terrain driving," *Mechanism Mach. Theory*, vol. 164, Oct. 2021, Art. no. 104368.

[14] M. J. Schuster *et al.*, "Towards autonomous planetary exploration," *J. Intell. Robot. Syst.*, vol. 93, no. 3, pp. 461–494, 2019.

[15] H. Kalita and J. Thangavelautham, "Automated multidisciplinary design and control of hopping robots for exploration of extreme environments on the moon and Mars," 2019, *arXiv:1910.03827*.

[16] F. Rosique, P. J. Navarro, C. Fernández, and A. Padilla, "A systematic review of perception system and simulators for autonomous vehicles research," *Sensors*, vol. 19, no. 3, p. 648, 2019.

[17] Y. Xu, J. Li, X. Lin, and F. Bai, "An optimal bit-rate allocation algorithm to improve transmission efficiency of images in deep space exploration," *China Commun.*, vol. 17, no. 7, pp. 94–100, Jul. 2020.

[18] T. Ling, L. Tao, W. Shimin, and L. Yafang, "The study of wheel driving torque optimization of Mars rover with active suspension in obstacle crossing," in *Proc. Int. Conf. Intell. Robot. Appl.* Cham, Switzerland: Springer, 2019, pp. 283–293.

[19] E. W. Schaler, J. Wisnowski, Y. Iwashita, J. A. Edlund, J. H. Sly, W. Raff, K. L. Kriechbaum, M. A. Frost, R. L. McCormick, and J. A. Townsend, "Two-stage calibration of a 6-axis force-torque sensor for robust operation in the Mars 2020 robot arm," *Adv. Robot.*, vol. 35, pp. 1–12, Nov. 2021.

[20] M. D'Antonio, C. Shi, B. Wu, and A. Khaligh, "Design and optimization of a solar power conversion system for space applications," *IEEE Trans. Ind. Appl.*, vol. 55, no. 3, pp. 2310–2319, Jun. 2019.

[21] *Home*. Accessed: Oct. 9, 2021. [Online]. Available: https://urc.marssociety.org/

[22] A. R. Jace, A. Tyler, K. Marc, and R. Michael. *BYU Mars Rover at The 2018*. Accessed: Dec. 3, 2021. [Online]. Available: https://repository.arizona.edu/bitstream/handle/10150/631687/ITC_2018_18-20-01.pdf?sequence=1

[23] T. Bernard, K. Martusevich, A. A. Rolins, I. Spence, A. Troshchenko, and S. Chintalapati, "A novel Mars rover concept for astronaut operational support on surface EVA missions," in *Proc. AIAA SPACE Astronaut. Forum Expo.* Reston, VA, USA: American Institute of Aeronautics and Astronautics, 2018, p. 5154.

[24] T. I. R. Uday, G. M. A. E. U. Rahman, F. S. Tithi, N. Ahmad, A. Ghosh, J. Jahin, M. Rahman, I. Iqbal, T. Islam, F. Farzana, and M. Rahman, "Design and implementation of the next generation Mars rover," in *Proc. 21st Int. Conf. Comput. Inf. Technol. (ICCIT)*, Dec. 2018, pp. 1–6.

[25] M. Gajewski, P. Cieplicka, L. Kostrzewa, and M. Hałoń. *Sirius—An Analog Mars Rover From SKA Robotics*. Accessed: Dec. 3, 2021. [Online]. Available: http://www.marspapers.org/paper/Gajewski_2019.pdf

[26] M. F. Khan, G. Wang, M. Z. A. Bhuiyan, and X. Li, "Wi-Fi signal coverage distance estimation in collapsed structures," in *Proc. IEEE Int. Symp. Parallel Distrib. Process. With Appl., IEEE Int. Conf. Ubiquitous Comput. Commun. (ISPA/IUCC)*, Dec. 2017, pp. 1066–1073.

[27] *Zed-Ros-Wrapper—ROS Wiki*. Accessed: Oct. 9, 2021. [Online]. Available: http://wiki.ros.org/zed-ros-wrapper

[28] *Robot_Localization—ROS Wiki*. Accessed: Oct. 9, 2021. [Online]. Available: http://wiki.ros.org/robot_localization

[29] *Rplidar_Ros—ROS Wiki*. Accessed: Oct. 9, 2021. [Online]. Available: http://wiki.ros.org/rplidar_ros

[30] *Gmapping—ROS Wiki*. Accessed: Oct. 9, 2021. [Online]. Available: http://wiki.ros.org/gmapping

[31] *Amcl—ROS Wiki*. Accessed: Oct. 9, 2021. [Online]. Available: http://wiki.ros.org/amcl

[32] *Move_Base—ROS Wiki*. Accessed: Oct. 9, 2021. [Online]. Available: http://wiki.ros.org/move_base

[33] *Nmea_Navsat_Driver—ROS Wiki*. Accessed: Oct. 9, 2021. [Online]. Available: http://wiki.ros.org/nmea_navsat_driver

[34] *Mapviz—ROS Wiki*. Accessed: Oct. 9, 2021. [Online]. Available: http://wiki.ros.org/mapviz

[35] *Gps_Goal—ROS Wiki*. Accessed: Oct. 9, 2021. [Online]. Available: http://wiki.ros.org/gps_goal

[36] *Ar_Track_Alvar—ROS Wiki*. Accessed: Oct. 9, 2021. [Online]. Available: http://wiki.ros.org/ar_track_alvar

[37] *Cmd_Vel_Mux—ROS Wiki*. Accessed: Oct. 9, 2021. [Online]. Available: http://wiki.ros.org/cmd_vel_mux

[38] *URC2020 Science Discussion*, Jun. 2020.

[39] C. Nielsen-Marsh, "Biomolecules in fossil remains: Multidisciplinary approach to endurance," *Biochemist*, vol. 24, no. 3, pp. 12–14, 2002.

[40] J. M. Oades, "Soil organic matter and structural stability: Mechanisms and implications for management," *Plant Soil*, vol. 76, nos. 1–3, pp. 319–337, Feb. 1984.

[41] F. M. Swain and M. A. Rogers, "Distribution of carbohydrate residues in some fossil specimens and associated sedimentary matrix and other geologic samples," *J. Sedimentary Res.*, vol. 37, no. 1, pp. 12–24, 1967.

[42] J. G. Palacas, F. M. Swain, and F. Smith, "Presence of carbohydrates and other organic compounds in ancient sedimentary rocks," *Nature*, vol. 185, no. 4708, p. 234, 1960.

[43] D. E. G. Briggs and R. E. Summons, "Ancient biomolecules: Their origins, fossilization, and role in revealing the history of life: Prospects & overviews," *BioEssays*, vol. 36, no. 5, pp. 482–490, May 2014.

[44] K. Simonyan and A. Zisserman, "Very deep convolutional networks for large-scale image recognition," 2014, *arXiv:1409.1556*.

[45] N. Vinod and H. E. Geoffrey, "Rectified linear units improve restricted Boltzmann machines," in *Proc. ICML*, 2010, pp. 807–814. [Online]. Available: https://icml.cc/Conferences/2010/papers/432.pdf

[46] S. Narayan, "The generalized sigmoid activation function: Competitive supervised learning," *Inf. Sci.*, vol. 99, nos. 1–2, pp. 69–82, Jun. 1997.

[47] D. P. Kingma and J. Ba, "Adam: A method for stochastic optimization," 2014, *arXiv:1412.6980*.

[48] A. K. Varma, B. Hazra, and A. Srivastava, "Estimation of total organic carbon in shales through color manifestations," *J. Natural Gas Sci. Eng.*, vol. 18, pp. 53–57, May 2014.

[49] P. V. Rich, *The Fossil Book: A Record of Prehistoric Life*. Mineola, NY, USA: Dover, 2020.

[50] *URC2020 Science Discussion*, Univ. Rover Challenge, Washington, DC, USA, Jun. 2020.

[51] J. Goordial, I. Altshuler, K. Hindson, K. Chan-Yam, E. Marcolefas, and L. G. Whyte, "*In situ* field sequencing and life detection in remote (79°26'N) Canadian high Arctic permafrost ice wedge microbial communities," *Frontiers Microbiol.*, vol. 8, Dec. 2017.

[52] M. Kiflen, O. Shariff, H. Mahdi, and F. Balsara, "Novel nucleic acid-based soil sample analysis system for planetary exploration," Dept. Mech. Process Eng., ETH Zürich, Rämistrasse, Zürich, Switzerland Tech. Rep., 2020, doi: 10.3929/ethz-b-000450123.

[53] M. F. Mora, F. Kehl, E. T. da Costa, N. Bramall, and P. A. Willis, "Fully automated microchip electrophoresis analyzer for potential life detection missions," *Anal. Chem.*, vol. 92, no. 19, pp. 12959–12966, 2020.

[54] A. Mojarro, G. Ruvkun, M. T. Zuber, and C. E. Carr, "Nucleic acid extraction from synthetic Mars analog soils for *in situ* life detection," *Astrobiology*, vol. 17, no. 8, pp. 747–760, Aug. 2017.

[55] E. S. Kite, E. Gaidos, and T. C. Onstott, "Valuing life-detection missions," *Astrobiology*, vol. 18, no. 7, pp. 834–840, 2018.

[56] M. Neveu, L. E. Hays, M. A. Voytek, M. H. New, and M. D. Schulte, "The ladder of life detection," *Astrobiology*, vol. 18, no. 11, pp. 1375–1402, 2018.

[57] M. Sharukh, B. Karim, S. Nv, and J. Thomas, "Intelligent deployable mini rover from the Mars rover for deep narrow scientific investigation," *Int. J. Sci. Res. Comput. Sci., Eng. Inf. Technol.*, vol. 5, pp. 174–184, May 2019.

AKIB ZAMAN received the B.Sc. degree in computer science and engineering from the Military Institute of Science and Technology (MIST), Dhaka, Bangladesh. He is currently a Lecturer at the Department of Computer Science and Engineering, United International University (UIU), Dhaka. He has experience in leading research works for premium robotics competitions like University Rover Challenge (URC) and U.K.-RAS Medical Robotics Challenge for contagious diseases. He is the author of six peer-reviewed publications in international journals and conferences. His research interests include robotics and autonomous systems, reinforcement learning, mining software repositories, image processing, and social computing.

MOHAMMAD SHAHJAHAN MAJIB received the B.Sc. degree in computer science and engineering from Dhaka University (DU), Dhaka, Bangladesh, the M.Sc. degree in computer science and engineering from the Military Institute of Science and Technology (MIST), Dhaka, and the Postgraduate Diploma degree in wired communication engineering from the PLA University of Science and Technology (PLAUST), China. He is currently working as a Senior Instructor with the Department of Computer Science and Engineering, MIST. His research interests include medical image processing, pattern recognition, and machine learning.

SHOEB AHMED TANJIM is currently pursuing the B.Sc. degree with the Department of Computer Science and Engineering, Military Institute of Science and Technology (MIST). His research interests include artificial intelligence, image processing, robotics, and the IoT.

SHAH MD. AHASAN SIDDIQUE received the B.Sc. degree in mechanical engineering from the Military Institute of Science and Technology (MIST), Dhaka. He is currently a Lecturer at the Department of Mechanical Engineering, Military Institute of Science and Technology (MIST). He has experience in research works for premium robotics competitions like University Rover Challenge (URC) and U.K.-RAS Medical Robotics Challenge for contagious diseases. He is also working on project of robotic arm for contour digitization. His research interests include robotics, machine design, computer-aided design, control systems, 3D printing, unmanned aerial vehicle, and automobile.

FARDEEN ASHRAF is currently pursuing the B.Sc. degree with the Department of Computer Science and Engineering, Military Institute of Science and Technology (MIST). His research interests include computer vision, natural language processing, robotics, and human–computer interaction.

SHAFAYETUL ISLAM is currently pursuing the B.Sc. degree with the Department of Computer Science and Engineering, Military Institute of Science and Technology (MIST). His research interests include artificial intelligence, image processing, robotics, and the IoT.

ABU HENA MD. MARUF MORSHED is currently pursuing the bachelor's degree with the Department of Mechanical Engineering, Military Institute of Science and Technology. He has experience in research work for premium robotics competition University Rover Challenge (URC). He is also working on a project of tendon driven robotic wrist. He is the author of one peer-reviewed publication in international conference based on his research on archimedes spiral wind turbine. His research interests include robotics, machine design, fluid mechanics, CFD, and renewable energy.

SHADMAN TAJWAR SHAHID is currently pursuing the B.Sc. degree with the Department of Mechanical Engineering, Military Institute of Science and Technology (MIST). His research interests include robotics, machine design, computer-aided design, and control systems.

ISHRAQ HASAN is currently pursuing the B.Sc. degree with the Department of Computer Science and Engineering, Military Institute of Science and Technology (MIST). His research interests include low-level system design, embedded systems, robotics, networking, and operating systems.

OLIULLAH SAMIR is currently pursuing the B.Sc. degree with the Department of Mechanical Engineering, Military Institute of Science and Technology (MIST). His research interests include robotics, machine design, nanotechnology, computer-aided design (CAD), and transport systems.

SAFWAN SHAFQUAT is currently pursuing the bachelor's degree with the Department of Mechanical Engineering, Military Institute of Science and Technology. He worked with multi-disciplinary teams in several national robotics competitions and in an international competition University Rover Challenge (URC) organized by the Mars Society. He is also working on a project on tendon driven robotic wrist. He is the author of one peer-reviewed publication in international conference based on his research on a rare wind turbine impact. His research interests include space exploration, sustainable energy, and technical drawing.

NAIM IBNA KHADEM AL BHUYAIN is currently pursuing the bachelor's degree in computer science and engineering with the Military Institute of Science and Technology. He has also competed in a number of national robotics contests. His research expertise is also featured in the robotics competition University Rover Challenge (URC). He is also working on a project involving the development of a contactless ATM system. He is the author of one peer-reviewed article at an international conference based on his research on stress classification using unsupervised machine learning approach. His research interests include image processing, human–computer interaction (HCI), and information technology (IT).

ASIF MAHMUD RAYHAN is currently pursuing the bachelor's degree with the Department of Mechanical Engineering, Military Institute of Science and Technology. He has experience in research work for premium robotics competition University Rover Challenge (URC). He is also working on a project on the delay of flow separation of an airfoil by applying different modifications. He is the author of one double-blind peer-reviewed publication in an international journal based on Natural fiber-based green bio-composites. His research interests include robotics, mechanical design, fluid mechanics, CFD, and materials and composites.

MD. MUSHFIK UL ISLAM is currently pursuing the B.Sc. degree with the Department of Mechanical Engineering, Military Institute of Science and Technology (MIST). His research interests include robotics, machine design, manufacturing technology, and engineering management.

MD. AKHTARUZZAMAN received the B.Sc. degree in computer science and engineering (CSE) from International Islamic University Chittagong (IIUC), Bangladesh, in 2005, and the M.Sc. degree in mechatronics engineering (MCT) and the Ph.D. degree in engineering (mechatronics & robotics) from the Kulliyyah of Engineering, International Islamic University Malaysia (IIUM), Malaysia, in 2012. During his professional career, he was a Programmer, a Software Engineer, and a Research Assistant. He is currently associated as an Assistant Professor with the Department of Computer Science and Engineering (CSE), Military Institute of Science and Technology (MIST), Dhaka, Bangladesh. He is also associated with DREAM Robotics Ltd., Dhaka, as a Consultant and a Research Scientist. He has published more than 48 research papers, including journals, conferences, books, and book chapters in artificial intelligence (AI), modeling and control, robotics, mechatronics system design, and communication engineering. His research interests include AI, modeling and control of mechatronics systems, robotics, rehabilitation engineering, computational musicology, algorithm design, and communication engineering.

MD. MAHBUBUR RAHMAN (Member, IEEE) received the Ph.D. degree in information computer science from the Japan Advanced Institute of Science and Technology (JAIST), Japan, in 2004. He is currently a Running Professor with the Department of Computer Science and Engineering (CSE), Military Institute of Science and Technology (MIST), Bangladesh. He has authored more than 75 research articles in reputed journals and conferences globally. His research interests include computer networks, image processing, pattern recognition, bioinformatics, and machine learning.

· · ·